Conclusion: Mucoepidermoid carcinoma of the bronchus is often visualized as marked heterogeneous contrast enhancement on HRCT images. The results of this study suggest that the presence of abundant microvessels, detected immunohistochemically by microscopic examination, affects the enhancement pattern on HRCT.

1. Introduction

Mucoepidermoid carcinoma of the lung is an extremely rare tumour, comprising less than 5% of primary bronchial tumours and 0.1–0.2% of all lung cancers [1–4]. The largest series (56 cases over 26 years) has been published by Yousem and Hochholzer [3]. These tumours are thought to originate from bronchial gland of minor salivary gland-type lining the bronchi, and are classified into low grade and high grade on the basis of histological criteria [1,3,5]. The most important factors in the prognosis include the histological grade and whether complete surgical resection is possible. Completely resectable low-grade tumours generally have an excellent prognosis [3,6].

The radiological appearance of mucoepidermoid carcinoma of the lung depends on tumour location, size and whether obstructive pneumonia is present. The reported computed tomographic (CT) appearance of mucoepidermoid carcinoma of the lung is a well circumscribed oval or lobulated mass arising within the bronchus [7]. Although some investigators have reported the CT features of this tumour [7–10], few reports have included detailed findings of high-resolution CT (HRCT) or correlated them with histopathologic features. The purpose of this study was to characterize the HRCT findings of mucoepidermoid carcinoma of the lung and correlate them with the histopathologic features.

2. Materials and methods

The patients investigated in this study presented at the National Cancer Center, Tokyo, Japan, for diagnosis and treatment during the period from January 1999 through December 2005. Only patients with primary mucoepidermoid carcinoma of the lung were included; patients with pulmonary metastasis from remote sites were excluded. Five patients underwent HRCT and were treated for primary mucoepidermoid carcinoma. The diagnosis was confirmed by histopathologic examination of the surgical specimen in all five patients. All clinical records, including the follow-up information, HRCT findings, endoscopic images and gross and microscopic specimens, were reviewed retrospectively.

2.1. HRCT protocols

HRCT was performed with either a 4-row or 16-row multi-detector CT (MDCT) scanner (Aquilion V-detector, Toshiba Medical Systems Corp., Tokyo Japan). The patients were evaluated with the MDCT scanner by using axial 2.0 mm × 4 mm or 16 modes, 120 kVp, 200–250 mA, and thin-section CT images were obtained using 1.0 mm sections reconstructed at 2.0 mm intervals with a high-spatial-frequency algorithm and retrospectively retargeted to each lung with a 20 cm field of view (FOV). All patients were intravenously injected with 80–150 ml of non-ionic contrast medium at a rate of 2.0–3.0 ml/s with an autoinjector (Autoenhance A-250, Nemoto Kyorindo, Tokyo, Japan), and scanning was started after a 40 s delay. Hard-copy images were photographed at window settings for the lung (center, −600 HU; width, 2000 HU) and the mediastinum (center, 35 HU; width, 400 HU). The intervals between the CT examinations and surgery ranged from 2 days to 4 weeks. All patients were followed up regularly in our institute. Follow-up CT images were obtained in all patients.

The HRCT images were assessed by two independent observers without reference to the clinical findings. The location of the pulmonary nodule was classified as peripheral or central. Nodules present within the peripheral two-thirds of the lung were arbitrarily classified as peripheral type and those within the central one-third or in contact with lobar or segmental bronchi were classified as central. The CT analysis included determination of the attenuation coefficient of the pulmonary lesion. CT attenuation coefficient was evaluated before and after administration of contrast media. The contrast enhancement of the tumour was compared with that of the chest wall musculature. Whether intratumoral calcification was present was also noted. After making independent initial evaluations, the two observers reviewed all cases in which their interpretations differed and reached a final consensus.

2.2. Histopathologic examination

Surgical specimens were inflated and fixed by transpleural and transbronchial infusion with formalin. The specimens were sectioned transversely in the same planes as the HRCT images, stained with hematoxylin-eosin and immunostained for the endothelial marker CD31. One of the authors, an experienced pulmonary pathologist, reviewed the histopathologic findings. The characteristics of the tumours on the HRCT images were compared with the histopathologic findings.

3. Results

3.1. Clinical features

The clinical data are summarized in Table 1. The five patients (two males and three females) ranged in age from 22 to 58 years, and their average age was 41.6 years. Only two of them were smokers. Four of the patients complained of chronic symptoms, including cough, increased sputum production and episodic fevers. These symptoms were related to bronchial irritation, partial or complete bronchial obstruction and distal pneumonia. The remain-

Please cite this article in press as: Ishizumi T, et al., Mucoepidermoid carcinoma of the lung: High-resolution CT and histopathologic findings in five cases, Lung Cancer (2007), doi:10.1016/j.lungcan.2007.08.022

Table 1 Clinical data of patients with mucoepidermoid carcinoma of the bronchus

Case	Age (year)	Sex	Symptom	Tumour location	Tumour site	Preoperative diagnosis
1	22	M	Cough, sputum	Central	Lt. LLB (B6)	Mucoepidermoid Ca.
2	40	W	Fever, chest pain	Central	Rt. MLB	Mucoepidermoid Ca.
3	58	W	Cough, sputum, fever	Central	Rt. BB (B9)	Non-typed malignant tumour
4	51	M	None	Peripheral	Rt. MLB (B4a)	No malignancy
5	37	W	Cough, sputum, fever	Central	Lt. UDB	No biopsy

Lt. LLB, Left lower lobe bronchus; Rt. BB, right basal bronchus; Rt. MLB, right middle lobe bronchus; Lt. UDB, left upper division bronchus.

ing patient was asymptomatic, and the lesion was detected during routine health examination.

The serum sialyl Lewis X-i antigen (SLX) values were high in all five cases. The serum carcinoembryonic antigen (CEA) and carbohydrate antigen 19-9 (CA19-9) values were high in three cases. The serum cytokeratin fragment 19 (CYFRA 21-1), squamous cell carcinoma antigen (SCC), neuron specific enolase (NSE), progastrin-releasing peptide (pro-GRP) values were all within the normal range.

3.2. HRCT findings

On the CT images, the tumours ranged in diameter from 18 to 38 mm (mean, 28.4 mm) (Table 2). The lesions were located in the central lung in four cases and in the peripheral lung in one. All the lesions were well defined nodules or masses with a smooth margin (Fig. 1). The contour of the tumours was round ($n=1$), oval ($n=3$) or lobulated ($n=1$). Non-enhanced CT scans revealed intratumoral punctate calcification in one of the five lesions (Case 1). CT findings suggestive of bronchial stenosis or obstruction were seen in all cases (distal obstructive pneumonia in four cases, distal bronchial dilation in four and atelectasis in three). Atelectasis with recurrent or non-resolving pneumonia was observed distal to the site of obstruction.

CT attenuation coefficients were evaluated before and after administration of contrast medium. Thus, the change of CT attenuation or the degree of contrast enhancement was described. CT images enhanced by intravenous contrast medium showed marked heterogeneous enhancement with foci of relatively low attenuation in four of the five lesions and mild heterogeneous enhancement in the other lesion. Measurement of Hounsfield unit (HU) data was possible in every patient. The attenuation coefficients of the four markedly enhanced tumours (range, 95–139 HU; mean, 118.5 HU) were much higher than those of the chest wall musculature (range, 48–68; mean, 61.3 HU), whereas that of the one mildly enhanced tumour was slightly higher than that of the chest wall musculature. The ratio of the attenuation coefficient of the tumour to that of the musculature in the mildly enhanced case was 1.5, whereas those of the markedly enhanced cases were much higher (range, 2.0–2.2) (Table 2). None of the patients had lymphadenopathy in the mediastinum, pulmonary hilum or around the bronchi, on the basis of the CT findings.

3.3. Bronchoscopic findings

Bronchoscopy was performed in all five cases and the tumours were easily visualized except the peripheral lesion. The tumours were located in the lobar or segmental bronchi and had filled the bronchial lumen. They were soft, polypoid with a sessile base and pink like the bronchial mucosa. Three of the tumours were covered by a highly vascular mucosa. Although bronchoscopic brushing or biopsy was performed in four cases, a preoperative diagnosis of mucoepidermoid carcinoma was made in only two of them. Bronchoscopy in the other two cases revealed a non-typed malignant tumour or non-diagnostic inflammatory cells.

3.4. Treatment

The treatment chosen for all patients was surgical resection, and the procedure consisted of routine lobectomy including right middle and lower lobectomy (Table 2). The surgical procedures resulted in tumour-free margins. Lymph node dissection or sampling of pulmonary hilar and mediastinal lymph nodes was performed in all cases.

3.5. Histopathologic findings

The histologic diagnosis was low-grade mucoepidermoid carcinoma in all five cases (Table 3). The central tumours

Table 2 HRCT findings of mucoepidermoid carcinoma of the bronchus in four patients

Case	Tumour size (mm)	Tumour margin	Tumour contour	Pattern of enhancement	Ratio of attenuation coefficient
1	38 × 35	Well defined (smooth)	Oval	Heterogeneous	2.1
2	26 × 18	Well defined (smooth)	Lobulated	Heterogeneous	1.5
3	34 × 22	Well defined (smooth)	Oval	Heterogeneous	2.1
4	24 × 24	Well defined (smooth)	Round	Heterogeneous	2
5	33 × 29	Well defined (smooth)	Oval	Heterogeneous	2.2

Ratio of attenuation coefficient: Ratio of the attenuation coefficient of the tumour to attenuation coefficient of the musculature

Please cite this article in press as: Ishizumi T, et al., Mucoepidermoid carcinoma of the lung: High-resolution CT and histopathologic findings in five cases, Lung Cancer (2007), doi:10.1016/j.lungcan.2007.08.022

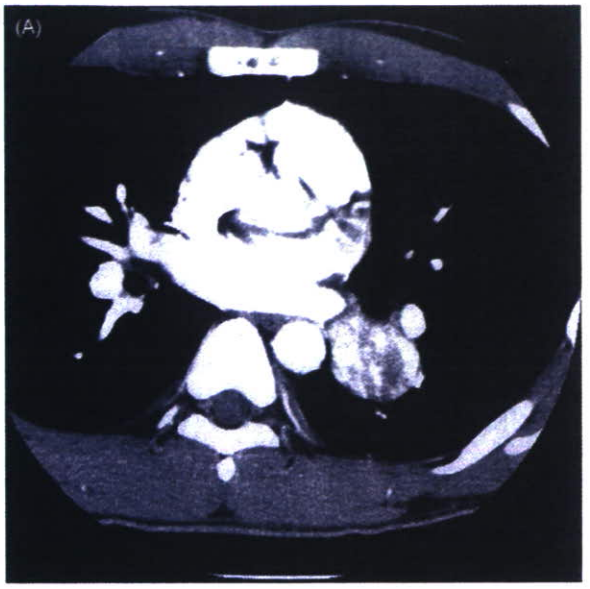

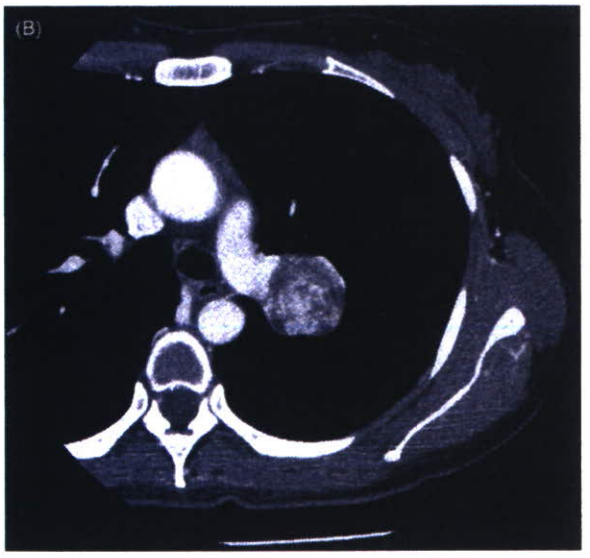

Fig. 1 Mucoepidermoid carcinomas of the bronchus were well defined mass and had a smooth margin. Enhanced CT images shows marked heterogeneous enhancement with foci of relatively low attenuation (A, Case 1; B, Case 5).

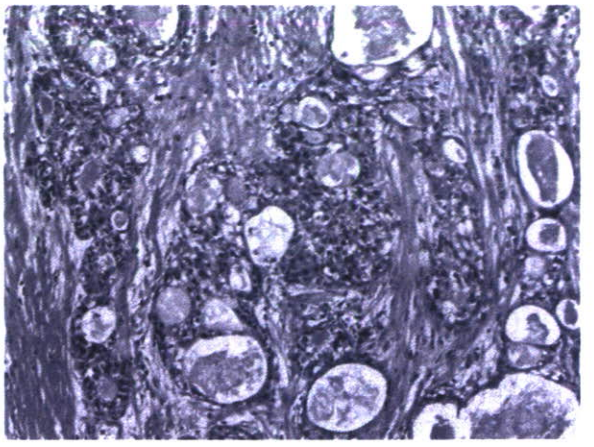

Fig. 2 High-magnification photomicrograph showed the epithelial component of the tumours consisted of mucin-secreting cells, squamoid cells and intermediate-type cells that displayed no specific differentiation.

protruded into the lumen of the bronchus and almost totally occluded it. On cut sections, the tumours were light yellow or tan polypoid masses. The margins and contours of the tumours were smooth, and they were well circumscribed and oval or round, consistent with their CT appearance.

Microscopically, the tumours were seen to arise from bronchial glands and to have infiltrated the bronchial wall. The epithelial component of the tumours consisted of mucin-secreting cells, squamoid cells and intermediate-type cells that displayed no specific differentiation (Fig. 2). Cystic change predominated in some areas, and the solid areas comprised mucin-secreting columnar epithelium that had formed small glands, tubules and cysts. There were no prominent nucleoli, and mitotic figures and necrosis were absent or minimal (less than five mitoses per 50 high-power fields). Keratinization was rare or absent in the epidermoid areas. These pathologic findings are characteristic of low-grade mucoepidermoid carcinoma. There was an admixed distribution of areas that are heterogeneous in the densities of blood vessels, as highlighted by immunohistochemical staining of CD31. Most mucin-secreting areas of the tumours showed more densely distributed blood vessels, mostly capillaries, in between tumour cell nests, whereas other areas did less (Fig. 3). Stromal calcification and ossification with a granulomatous reaction was observed in Case 1. The histologic specimens in Case 1, in which intratumoral punctate calcifications were observed on non-enhanced HRCT scans, showed microscopic calcification. Distal obstructive pneu-

Table 3 Histopathologic findings and outcome

Case	Treatment	p-Stage (TNM)	Grade	CD31	Outcome
1	Left lower lobectomy	T2N0M0 IB	Low-grade	(++)	NED
2	Right middle and lower lobectomy	T1N0M0 IA	Low-grade	(++)	NED
3	Right lower lobectomy	T2N0M0 IB	Low-grade	(+)	NED
4	Right middle lobectomy	T1N0M0 IA	Low-grade	(++)	NED
5	Light upper lobectomy	T2N0M0 IB	Low-grade	(++)	NED

NED: No evidence of disease.

Please cite this article in press as: Ishizumi T, et al., Mucoepidermoid carcinoma of the lung: High-resolution CT and histopathologic findings in five cases, Lung Cancer (2007), doi:10.1016/j.lungcan.2007.08.022

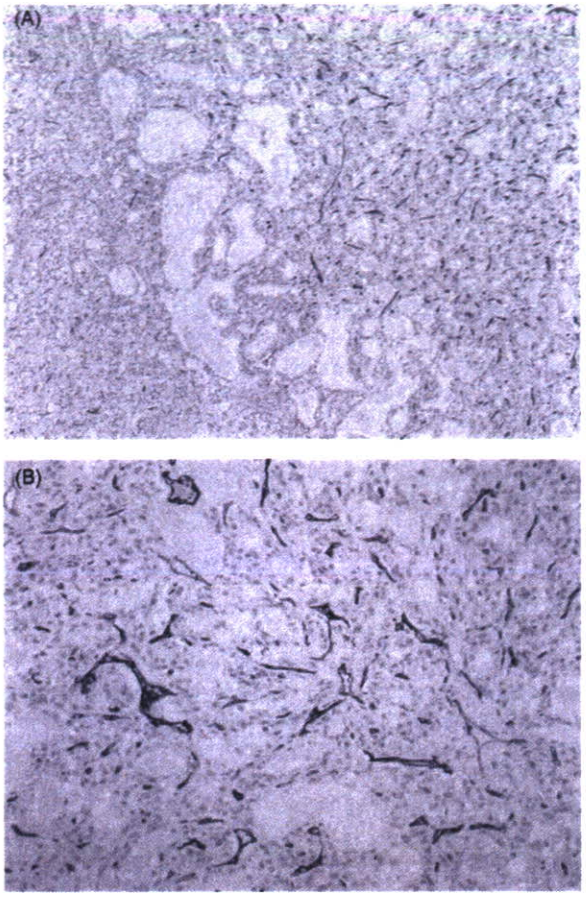

Fig. 3 (A) Immunohistochemical findings showing a border of areas with and without dense blood vessels as highlighted by anti-CD31 antibody. Note the abundant glands with mucus production in the right half, where there are more vessels labeled by anti-CD31 antibody. (B) Higher magnification of the area with plenty of mucin-secreting glands. Immunoreactive CD31 label the surface of endothelial cells, but not mucin of the tumour.

monia was observed in four patients with lesions of the central type, and distal bronchial dilation and mucoid impaction was seen in all five cases. The secondary findings associated with bronchial stenosis or obstruction on the HRCT scans largely reflected these pathologic findings. No lymph node metastasis was found in any of the surgical specimens.

4. Discussion

Mucoepidermoid carcinoma of the lung was first reported by Smetana et al. [11], and accounts for only a very small proportion of primary lung cancers. The tumours are classified as low grade or high grade based on their histologic appearance, and grading is based on cellular atypia, mitotic activity, local extension and tumour necrosis. Low-grade mucoepidermoid carcinoma is the most common type, and all five of the tumours in our series were low-grade. Although there is good clinicopathological evidence for the existence of the low-grade type, it has been questioned whether the high-grade type is a separate entity, mainly because of its histological similarity to mixed pulmonary carcinomas [5]. The high-grade variant is occasionally difficult to differentiate from adenosquamous carcinoma [12–14].

The most common symptoms are related to intraluminal growth, and these include persistent cough and sputum, wheezing, dyspnea, recurrent pneumonia, and, less frequently, hemoptysis [15]. Since the symptoms do not differ from those of other forms of lung tumour, they do not contribute to the differential diagnosis. Most patients with mucoepidermoid carcinoma are misdiagnosed as having bronchitis or lung carcinomas of other types. In our series, one patient was asymptomatic and the others had such similar symptoms that they were initially misdiagnosed as having chronic obstructive airway disease or other airway tumours.

Although the central-type tumours in our series were readily visible, only two of them were diagnosed preoperatively as mucoepidermoid carcinoma. Since mucoepidermoid carcinomas of the bronchi are usually covered by normal respiratory mucosa, bronchial brushing and lavage are seldom diagnostic, and it is better to perform a biopsy with forceps. Despite the theoretical risk of severe hemorrhage by performing a biopsy on a vascular mass, hemorrhage has never been reported as a complication of biopsy for mucoepidermoid carcinoma of the bronchus. Nevertheless, care is required because of the highly vascular nature of many of the tumours.

CT scan is non-invasive and useful for evaluating suspected endobronchial lesions, and fine morphological features have been revealed since the introduction of HRCT. In this series, HRCT images were essential for identifying the more detailed characteristics of the tumours, such as the margin, shape, density and pattern of enhancement. For the most part, the HRCT images reflected the pathologic features of the tumours well. There have been a few case reports of the HRCT appearance of mucoepidermoid carcinoma of the lung [7,10]. The HRCT features of the tumours in our series, such as a smooth margin and a well defined oval or round shape, were similar to those reported by Kim et al., who also found intratumoral punctate calcification on non-enhanced CT scans. Secondary findings associated with bronchial stenosis or obstruction, such as distal obstructive pneumonia, bronchial dilatation and atelectasis, were also seen. Although in their series Kim et al. reported mucoepidermoid carcinoma of the bronchus as showing mild contrast enhancement on CT scans, the three lesions of the central type and one lesion of the peripheral type in our series demonstrated marked contrast enhancement on HRCT images. The attenuation coefficients of the markedly enhanced tumours were much higher than those of the chest wall musculature.

Immunohistochemical staining for CD31 highlighted the heterogeneous distribution of blood vessels from mucin-secreting areas to non-secreting areas in a single tumour. In other words, these lesions may have characteristics of both hypervascular and hypovascular components, and the presence of both was probably the explanation for the features we observed on HRCT. The results of this study suggested that the presence of abundant microvessels, detected immunohistochemically by microscopic examination, affected the enhancement pattern on HRCT. These histopathologic findings correlated with the HRCT findings in all patients.

Please cite this article in press as: Ishizumi T, et al., Mucoepidermoid carcinoma of the lung: High-resolution CT and histopathologic findings in five cases, Lung Cancer (2007), doi:10.1016/j.lungcan.2007.08.022

Bronchogenic carcinomas with more common histologic features, including adenocarcinoma, squamous cell carcinoma and small cell carcinoma have a variety of radiologic manifestations. Adenocarcinoma is often distinct from the other histologic subtypes of lung cancer. Non-solid nodules (ground glass opacities) and partly solid nodules (mixed solid/ground glass opacities) are recognized patterns of adenocarcinoma. Henschke et al. reported that the malignancies in subsolid nodules were typically bronchioloalveolar carcinomas or adenocarcinomas with bronchioloalveolar features, whereas in solid ones the malignancies were typically other subtypes of adenocarcinoma [16]. The proportion occupied by the non-solid component based on volumetric analysis by CT scan is a reliable predictor of tumours without vessel invasion in patients with adenocarcinoma of the lung [17]. Central squamous cell carcinoma is characterized by two major patterns of spread: intraepithelial spread with or without subepithelial invasion, and endobronchial polypoid growth. Polypoid tumours often occlude the bronchial lumen, resulting in atelectasis and obstructive pneumonia. Peripheral squamous cell carcinomas are seen as solid nodules, occasionally with cavitation and irregular margins. Approximately 90–95% of all small cell lung cancers are located centrally and show mediastinal or hilar lymphadenopathy with displacement or narrowing of the tracheobronchial tree or major vessels [18]. These common histologic types of lung cancer usually show mild or less contrast enhancement on CT images. Since these CT findings in common forms of lung carcinoma differ from those of mucoepidermoid carcinoma, which are relatively characteristic, contrast-enhanced CT may be helpful for lesion characterization and tumour classification in affected patients. If a marked heterogeneous contrast enhancement pattern is observed in well circumscribed oval or round masses of the bronchus, mucoepidermoid carcinoma can be considered in the differential diagnosis.

Large cell neuroendocrine carcinoma shows non-specific CT findings similar to those of other non-small cell lung cancer. On contrast-enhanced CT scans, tumour attenuation varies from slightly less to more than that of the chest wall muscle, with a homogeneous or heterogeneous pattern [18,19]. However, large cell neuroendocrine carcinoma is more likely to appear in the peripheral lung. Adenosquamous carcinoma of the peripheral type also usually shows heterogeneous soft-tissue attenuation [20]. Histopathologically, adenosquamous carcinoma is occasionally difficult to differentiate from high-grade mucoepidermoid carcinoma, which invades the pulmonary parenchyma in nearly 46% of the cases [3,12–14].

Pulmonary carcinoid tumours, which are low-grade malignancies accounting for 2–3% of all lung neoplasms [21], show CT findings similar to those of mucoepidermoid carcinoma. Pulmonary carcinoid tumours are also known to be vascular, and often show marked contrast enhancement on CT images [18,22]. Therefore, it is difficult to differentiate pulmonary carcinoid tumour from mucoepidermoid carcinoma on the basis of the CT contrast enhancement pattern alone.

Follow-up information was available for all five of the present cases. The clinical course of the patients was correlated with the histologic grade of their tumours. Low-grade mucoepidermoid carcinoma generally grows locally and is amenable to complete surgical resection. Low-grade tumours spread to regional lymph nodes by local growth in less than 5% of cases, and distant spread is rare [3,15]. The prognosis of low-grade tumours is usually excellent, with no evidence of local recurrence or metastasis. However, Barsky et al. [23] reported cases that were diagnosed as well differentiated and low-grade malignancy histologically but were rated as high-grade malignancy clinically. It can therefore be concluded that the histologic malignancy level of the tumour is not always the same as its clinical malignancy level. This suggests that complete surgical resection plus lymph node dissection should be performed for low-grade mucoepidermoid carcinoma of the bronchus as well as high-grade mucoepidermoid carcinoma. All five patients in our series underwent lobectomy plus lymph node dissection or sampling, and all are currently alive without evidence of disease at an average of 50.4 months after surgery (range, 15–82 months; median, 57 months).

5. Conclusions

We reviewed the HRCT and pathologic findings in five cases of mucoepidermoid carcinoma of the lung. Mucoepidermoid carcinoma is often visualized as marked heterogeneous contrast enhancement on HRCT images. The presence of abundant microvessels, detected immunohistochemically by microscopic examination, may affect the enhancement pattern on HRCT. However, examinations of HRCT images of mucoepidermoid carcinoma of the lung are insufficient because of the rarity of the tumour. The HRCT characteristics of the tumour must therefore be evaluated in more cases.

Conflict of interest

None declared.

References

[1] Colby TV, Koss MN, Travis WD. Tumors of salivary gland type. Tumors of the lower respiratory tract: AFIP atlas of tumor pathology 3rd series, vol. 13. Washington, DC: American Registry of Pathology; 1995. p. 65–89.
[2] Spencer H. Bronchial mucous gland tumours. Virchows Arch A Pathol Pathol Anat 1979;383:101–15.
[3] Yousem SA, Hochholzer L. Mucoepidermoid tumors of the lung. Cancer 1987;60:1346–52.
[4] Miller DL, Allen MS. Rare pulmonary neoplasms. Mayo Clin Proc 1993;68:492–8.
[5] Klacsmann PG, Olson JL, Eggleston JC. Mucoepidermoid carcinoma of the bronchus: an electron microscopic study of the low grade and the high grade variants. Cancer 1979;43:1720–33.
[6] Heitmiller RF, Mathisen DJ, Ferry JA, Mark EJ, Grillo HC. Mucoepidermoid lung tumors. Ann Thorac Surg 1989;47:394–9.
[7] Kim TS, Lee KS, Han J, Im JG, Seo JB, Kim JS, et al. Mucoepidermoid carcinoma of the tracheo-bronchial tree: radiographic and CT findings in 12 patients. Radiology 1999;212:643–8.
[8] Fisher DA, Mond DJ, Fuchs A, Khan A. Mucoepidermoid tumor of the lung: CT appearance. Comput Med Imaging Graph 1995;19:339–42.

Please cite this article in press as: Ishizumi T, et al., Mucoepidermoid carcinoma of the lung: High-resolution CT and histopathologic findings in five cases, Lung Cancer (2007), doi:10.1016/j.lungcan.2007.08.022

[9] Tsuchiya H, Nagashima K, Ohashi S, Takase Y. Childhood bronchial mucoepidermoid tumors. J Pediatr Surg 1997;32:106–9.
[10] Kinoshita H, Shimotake T, Furukawa T, Deguchi E, Iwai N. Mucoepidermal carcinoma of the lung detected by positron emission tomography in a 5-year-old girl. J Pediatr Surg 2005;40:E1–3.
[11] Smetana HF, Iverson L, Swan LL. Bronchogenic carcinoma. Analysis of 100 autopsy cases. Milit Surg 1952;3:335–51.
[12] Leonardi HK, Jung-Legg Y, Legg MA, Neptune WB. Tracheobronchial mucoepidermoid carcinoma: clinicopathological features and results of treatment. J Thorac Cardiovasc Surg 1978;76:431–8.
[13] Stafford JR, Pollock J, Wenzel BC. Oncocytic mucoepidermoid tumor of the bronchus. Cancer 1984;54:94–9.
[14] Stafford JR, Pollock J, Wenzel BC. Bronchial mucoepidermoid carcinoma metastatic to skin. Report of a case and review of the literature. Cancer 1986;58:2556–9.
[15] Granata C, Battistini E, Toma P, Balducci T, Mattioli G, Fregonese B, et al. Mucoepidermoid carcinoma of the bronchus. Paediatr Pulmonol 1997;23:226–32.
[16] Henschke CI, Yankelevitz DF, Mirtcheva R, McGuinness G, McCauley D, Miettinen OS, et al. CT screening for lung cancer: frequency and significance of part-solid and nonsolid nodules. AJR Am J Roentgenol 2002;178:1053–7.
[17] Tateishi U, Uno H, Yonemori K, Satake M, Takeuchi M, Arai Y. Prediction of lung adenocarcinoma without vessel invasion: a CT scan volumetric analysis. Chest 2005;128:3276–83.
[18] Chong S, Lee KS, Chung MJ, Han J, Kwon OJ, Kim TS. Neuroendocrine tumors of the lung: clinical, pathologic, and imaging findings. Radiographics 2006;26:41–57.
[19] Oshiro Y, Kusumoto M, Matsuno Y, Asamura H, Tsuchiya R, Terasaki H, et al. CT findings of surgically resected large cell neuroendocrine carcinoma of the lung in 38 patients. AJR Am J Roentgenol 2004;182:87–91.
[20] Yu JQ, Yang ZG, Austin JH, Guo YK, Zhang SF. Adenosquamous carcinoma of the lung: CT-pathological correlation. Clin Radiol 2005;60:364–9.
[21] Davila DG, Dunn WF, Tazelaar HD, Pairolero PC. Bronchial carcinoid tumors. Mayo Clin Proc 1993;68:795–803.
[22] Fauroux B, Aynie V, Larroquet M, Boccon-Gibod L, Ducou le Pointe H, Tamalet A, et al. Carcinoid and mucoepidermoid bronchial tumours in children. Eur J Pediatr 2005;164:748–52.
[23] Barsky SH, Martin SE, Matthews M, Gazdar A, Costa JC. "Low grade" mucoepidermoid carcinoma of the bronchus with "high grade" biological behavior. Cancer 1983;51:1505–9.

Please cite this article in press as: Ishizumi T, et al., Mucoepidermoid carcinoma of the lung: High-resolution CT and histopathologic findings in five cases, Lung Cancer (2007), doi:10.1016/j.lungcan.2007.08.022

British Journal of Cancer (2008) 98, 693–696

www.bjcancer.com

Short Communication

Randomised phase II trial of irinotecan plus cisplatin *vs* irinotecan, cisplatin plus etoposide repeated every 3 weeks in patients with extensive-disease small-cell lung cancer

I Sekine*[,1], H Nokihara[1], K Takeda[2], Y Nishiwaki[3], K Nakagawa[4], H Isobe[5], K Mori[6], K Matsui[7], N Saijo[3] and T Tamura[1]

[1]Division of Internal Medicine and Thoracic Oncology, National Cancer Center Hospital, Tokyo, Japan; [2]Department of Clinical Oncology, Osaka City General Hospital, Osaka, Japan; [3]Division of Thoracic Oncology, National Cancer Center Hospital East, Kashiwa, Japan; [4]Department of Medical Oncology, Kinki University School of Medicine, Sayama, Japan; [5]Department of Pulmonary Disease, National Hospital Organization Hokkaido Cancer Center, Sapporo, Japan; [6]Department of Thoracic Diseases, Tochigi Prefectural Cancer Center, Utsunomiya, Japan; [7]Department of Internal Medicine, Osaka Prefectural Medical Center for Respiratory and Allergic Diseases, Habikino, Japan

Patients with previously untreated extensive-disease small-cell lung cancer were treated with irinotecan 60 mg m^{-2} on days 1 and 8 and cisplatin 60 mg m^{-2} on day 1 with ($n = 55$) or without ($n = 54$) etoposide 50 mg m^{-2} on days 1–3 with granulocyte colony-stimulating factor support repeated every 3 weeks for four cycles. The triplet regimen was too toxic to be considered for further studies.

British Journal of Cancer (2008) **98**, 693–696. doi:10.1038/sj.bjc.6604233 www.bjcancer.com
Published online 5 February 2008

Keywords: small-cell lung cancer; chemotherapy; irinotecan; etoposide; three drug combination

Small-cell lung cancer (SCLC), which accounts for approximately 14% of all malignant pulmonary tumours, is an aggressive malignancy with a propensity for rapid growth and early widespread metastases (Jackman and Johnson, 2005). A combination of cisplatin and etoposide (PE) has been the standard treatment, with response rates ranging from 60 to 90% and median survival times (MSTs) from 8 to 11 months in patients with extensive disease (ED)-SCLC (Fukuoka *et al*, 1991; Roth *et al*, 1992). A combination of irinotecan and cisplatin (IP) showed a significant survival benefit over the PE regimen (MST: 12.8 *vs* 9.4 months, $P = 0.002$) in a Japanese phase III trial for ED-SCLC (Noda *et al*, 2002), although another phase III trial comparing these regimens failed to show such a benefit (Hanna *et al*, 2006). Thus, irinotecan, cisplatin and etoposide are the current key agents in the treatment of SCLC. A phase II trial of the three agents, IPE combination, in patients with ED-SCLC showed a promising antitumour activity with a response rate of 77%, complete response (CR) rate of 17% and MST of 12.9 months (Sekine *et al*, 2003).

We have developed these IP and IPE regimens in a 4-week schedule where irinotecan was given on days 1, 8 and 15. The dose of irinotecan on day 15, however, was frequently omitted because of toxicity in both regimens (Noda *et al*, 2002; Sekine *et al*, 2003). The objectives of this study were to evaluate the toxicities and antitumour effects of IP and IPE regimens in the 3-week schedule in patients with ED-SCLC and to select the right arm for subsequent phase III trials.

*Correspondence: Dr I Sekine, Division of Internal Medicine and Thoracic Oncology, National Cancer Center Hospital, Tsukiji 5-1-1, Chuo-ku, Tokyo 104-0045, Japan; E-mail: isekine@ncc.go.jp
Received 15 October 2007; revised 2 January 2008; accepted 9 January 2008; published online 5 February 2008

PATIENTS AND METHODS

Patient selection

Patients were enrolled in this study if they met the following criteria: (1) a histological or cytological diagnosis of SCLC; (2) no prior treatment; (3) measurable disease; (4) ED, defined as having distant metastasis or contralateral hilar lymph node metastasis; (5) performance status of 0–2 on the Eastern Cooperative Oncology Group (ECOG) scale; (6) predicted life expectancy of 3 months or longer; (7) age between 20 and 70 years; (8) adequate organ function as documented by a white blood cell (WBC) count $\geqslant 4.0 \times 10^3\,\mu l^{-1}$, neutrophil count $\geqslant 2.0 \times 10^3\,\mu l^{-1}$, haemoglobin $\geqslant 9.5\,g\,dl^{-1}$, platelet count $\geqslant 100 \times 10^3\,\mu l^{-1}$, total serum bilirubin $\leqslant 1.5\,mg\,dl^{-1}$, hepatic transaminases $\leqslant 100\,IU\,l^{-1}$, serum creatinine $\leqslant 1.2\,mg\,dl^{-1}$, creatinine clearance $\geqslant 60\,ml\,min^{-1}$, and $PaO_2 \geqslant 60$ torr; and (9) providing written informed consent.

Patients were not eligible for the study if they had any of the following: (1) uncontrollable pleural, pericardial effusion or ascites; (2) symptomatic brain metastasis; (3) active infection; (4) contraindications for the use of irinotecan, including diarrhoea, ileus, interstitial pneumonitis and lung fibrosis; (5) synchronous active malignancies; (6) serious concomitant medical

Clinical Studies

illness, including severe heart disease, uncontrollable diabetes mellitus or hypertension; or (7) pregnancy or breast feeding.

Treatment schedule

In the IP arm, cisplatin, 60 mg m^{-2}, was administered intravenously over 60 min on day 1 and irinotecan, 60 mg m^{-2}, was administered intravenously over 90 min on days 1 and 8. Prophylactic granulocyte colony-stimulating factor (G-CSF) was not administered in this arm. In the IPE arm, cisplatin and irinotecan were administered at the same dose and schedule as the IP arm. In addition, etoposide, 50 mg m^{-2}, was administered intravenously over 60 min on days 1–3. Filgrastim 50 μg m^{-2} or lenograstim 2 μg kg^{-1} was subcutaneously injected prophylactically from day 5 to the day when the WBC count exceeded 10.0×10^3 μl^{-1}. Hydration (2500 ml) and a $5HT_3$ antagonist were given on day 1, followed by an additional infusion if indicated in both arms. These treatments were repeated every 3 weeks for a total of four cycles.

Toxicity assessment, treatment modification and response evaluation

Toxicity was graded according to the NCI Common Toxicity Criteria version 2.0.

Doses of anticancer agents in the following cycles were modified according to toxicity in the same manner in both arms. Objective tumour response was evaluated according to the Response Evaluation Criteria in Solid Tumors (RECIST) (Therasse *et al*, 2000).

Study design, data management and statistical considerations

This study was designed as a multi-institutional, prospective randomised phase II trial. This study was registered on 6 September 2005 in the University hospital Medical Information Network (UMIN) Clinical Trials Registry in Japan (http://www.umin.ac.jp/ctr/index.htm), which is acceptable to the International Committee of Medical Journal Editors (ICMJE) (http://www.icmje.org/faq.pdf). The protocol and consent form were approved by the Institutional Review Board of each institution. Patient registration and randomisation were conducted at the Registration Center. No stratification for randomisation was performed in this study. The sample size was calculated according to the selection design for pilot studies based on survival (Liu *et al*, 1993). Assuming that (1) the survival curve was exponential for survivals; (2) the MST of the worse arm was 12 months and that of the better arm was 12 months × 1.4; (3) the correct selection probability was 90%; and (4) additional follow-up in years after the end of accrual was 1 year, the estimated required number of patients was 51 for each arm. Accordingly, 55 patients for each arm and their accrual period of 24 months were planned for this study.

The dose intensity of each drug was calculated for each patient using the following formula as previously described:

$$\text{The dose intensity (mg m}^{-2}\text{ week}^{-1}\text{)} = \frac{\text{Total milligrams of a drug in all cycles per body surface area}}{\text{Total days of therapy}/7}$$

where total days of therapy is the number of days from day 1 of cycle 1 to day 1 of the last cycle plus 21 days for both arms (Hryniuk and Goodyear, 1990).

Differences in the reason for termination of the treatment and the frequencies of grade 3–4 toxicities were assessed by χ tests. Survival was measured as the date of randomisation to the date of death from any cause or the date of the most recent follow-up for overall survival and to the date of disease progression or the date of death for progression-free survival (PFS). The survival of the arms was estimated by the Kaplan–Meier method and compared in an exploratory manner with log-rank tests (Armitage *et al*, 2002).

RESULTS

Patient characteristics

From March 2003 to May 2005, 55 patients were randomised to IP and 55 patients to IPE. One patient in the IP arm was excluded because the patient was ineligible and did not receive the study treatment. The remaining 109 patients were included in the analyses of toxicity, tumour response and patient survival. There were no differences between the two arms in any demographic characteristics listed (Table 1).

Treatment delivery

Treatment was well tolerated with respect to the number of cycles delivered in both arms (Table 2). Among reasons for termination of the treatment, disease progression was noted in nine (17%)

Table 1 Patient characteristics

	IP ($n=54$)	IPE ($n=55$)
Sex		
Female	11	8
Male	43	47
Age (years)		
Median (range)	63 (42–70)	62 (48–70)
PS		
0	11	12
1	42	41
2	1	2
Weight loss		
0–4%	38	43
5–9%	10	10
⩾10%	6	2

Table 2 Treatment delivery

	IP ($n=54$) No. (%)	IPE ($n=55$) No. (%)
Number of cycles delivered		
6[a]	—	1 (2)
4	41 (76)	36 (65)
3	6 (11)	6 (11)
2	3 (6)	6 (11)
1	4 (7)	6 (11)
Reasons for termination of the treatment[†]		
Completion	40 (74)	35 (64)
Disease progression	9 (17)	2 (4)
Toxicity	3 (6)	13 (24)
Patient refusal	2 (4)	4 (7)
Others	0 (0)	1 (2)
Total number of cycles delivered	192 (100)	186 (100)
Total number of omission on day 8	35 (18)	37 (17)
Total number of cycles with dose reduction	28 (15)	31 (17)

[†]$P=0.013$ by χ^2 test. [a]Protocol violation.

patients in the IP arm and in two (4%) patients in the IPE arm, whereas toxicity was noted in three (6%) patients in the IP arm and 13 (24%) patients in the IPE arm ($P=0.013$) (Table 2). The dose of irinotecan on day 8 was omitted in 35 (18%) cycles in the IP arm and 37 (17%) cycles in the IPE arm (Table 2). The total dose and dose intensity of cisplatin and etoposide were similar between the IP and IPE arms in the present study (Table 3).

Toxicity

The myelotoxicity was more severe in the IPE arm (Table 4). Grade 3 febrile neutropaenia was noted in 5 (9%) patients in the IP arm and 17 (31%) patients in the IPE arm ($P=0.005$). Packed red blood cells were transfused in 4 (7%) patients in the IP regimen and 14 (26%) patients in the IPE regimen ($P=0.011$). Platelet concentrates were needed in none in the IP regimen and 2 (4%) patients in the IPE regimen ($P=0.16$). Grade 3–4 diarrhoea was observed in 8 (15%) patients in the IP arm and 13 (24%) patients in the IPE arm ($P=0.262$). Grade 3–4 fatigue was more common in the IPE arm with marginal significance (2 *vs* 11%, $P=0.054$). The severity of other non-haematological toxicities did not differ significantly between the arms. No treatment-related death was observed in this study.

Table 3 Total dose and dose intensity

	3-week regimens in this study		4-week regimen[a]
	IP ($n=54$) Median (range)	IPE ($n=55$) Median (range)	IPE ($n=30$) Median (range)
Total dose ($mg\,m^{-2}$)			
Cisplatin	240 (60–240)	240 (60–360)	240 (60–240)
Irinotecan	420 (60–480)	390 (60–720)	563 (60–720)
Etoposide	0	600 (150–900)	600 (150–600)
Dose intensity ($mg\,m^{-2}\,week^{-1}$)			
Cisplatin	19 (14–25)	20 (16–34)	15 (12–15)
Irinotecan	33 (14–40)	35 (15–55)	35 (19–45)
Etoposide	0	48 (34–68)	37 (28–38)

[a]From our previous study (Sekine *et al*, 2003).

Table 4 Grade 3–4 toxicities

	IP ($n=54$)			IPE ($n=55$)		
	Grade 3	4	3+4 (%)	Grade 3	4	3+4 (%)
Leukocytopaenia	9	1	10 (19)	18	11	29 (53)*
Neutropaenia	17	11	28 (52)	24	28	52 (95)*
Anaemia	18	0	18 (25)	16	9	25 (45)
Thrombocytopaenia	2	0	2 (4)	13	0	13 (13)†
Febrile neutropaenia	5	0	5 (9)	17	0	7 (13)
Diarrhoea	8	0	8 (15)	11	2	13 (24)
Vomiting	4	0	4 (7)	3	0	3 (5)
Fatigue	1	0	1 (2)	5	1	6 (11)‡
Hyponatraemia	9	3	12 (22)	11	2	13 (24)
AST elevation	0	0	0 (0)	3	0	3 (5)
CRN elevation	1	0	1 (2)	0	0	0 (0)

*$P<0.001$; †$P<0.01$; and ‡$P=0.054$ by χ^2 test.

Response, treatment after recurrence and survival

Four CRs and 37 partial responses (PRs) were obtained in the IP arm, resulting in the overall response rate of 76 with 95% confidence interval (CI) of 65–87%, whereas six CRs and 42 PRs were obtained in the IPE arm, and the overall response rate was 87% with a 95% CI of 79–96% ($P=0.126$). Median PFS was 4.8 months (95% CI, 4.0–5.6) in the IP and 5.4 months (95% CI, 4.8–6.0) in the IPE arm ($P=0.049$) (Figure 1A). After recurrence, 22 (44%) patients in the IP arm and 8 (16%) patients in the IPE arm received etoposide-containing chemotherapy. The MST and 1-year survival rate were 12.4 months (95% CI, 9.7–15.1) and 54.8% (95% CI, 41.4–68.2%) in the IP and 13.7 months (95% CI, 11.9–15.5) and 61.5% (95% CI, 48.6–74.4%) in the IPE arm ($P=0.52$), respectively (Figure 1B).

DISCUSSION

This study showed that the IPE regimen in a 3-week schedule with CSF support produced a promising response rate, PFS and overall survival. Haematological toxicity in the IPE arm, however, was very severe in spite of the G-CSF support with the grade 3 febrile neutropaenia noted in 31% of patients.

In comparison between the 3-week IPE regimen in this study and the 4-week IPE regimen in the previous study, the delivery of cisplatin and etoposide was improved in the 3-week IPE regimen when compared with the 4-week IPE regimen at the cost of the irinotecan total dose. The response rate and MST were 87% and 13.7 months, respectively, in the 3-week IPE regimen and 77% and 12.9 months in the previous 4-week schedule, and toxicity profiles were comparable to each other (Sekine *et al*, 2003).

The MST of 12.4 months in the IP arm in this study was comparable to that of the previous phase III study, with an MST of 12.8 months (Noda *et al*, 2002). Thus, this study showed the reproducible excellent survival outcome of patients with ED-SCLC who were treated with the IP combination. In contrast, a recent American phase III study of the PE regimen *vs* IP regimen failed to show the superiority of the IP regimen to the PE regimen; the MST

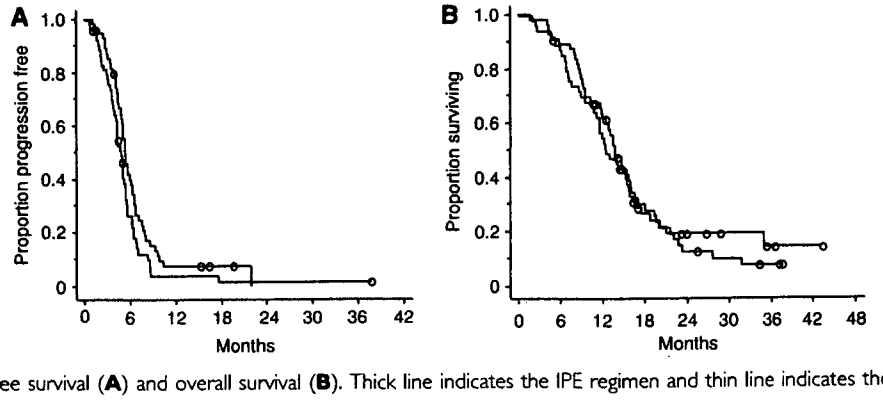

Figure 1 Progression-free survival (**A**) and overall survival (**B**). Thick line indicates the IPE regimen and thin line indicates the IP regimen.

for the PE regimen was 10.2 months and that for the IP regimen was 9.3 months (Hanna *et al*, 2006). The discrepancy between the Japanese and American trials may be explained by the different cisplatin dose schedules; cisplatin was delivered at a dose of $60\,mg\,m^{-2}$ on day 1 every 3 or 4 weeks in the Japanese trials, whereas cisplatin was delivered at a dose of $30\,mg\,m^{-2}$ on days 1 and 8 every 3 weeks in the American one. A platinum agent administered at divided doses was associated with poor survival in patients with ED-SCLC in our previous randomised phase II study (Sekine *et al*, 2003).

The issue of adding further agents to the standard doublet regimen has been investigated in patients with ED-SCLC. The addition of ifosfamide or cyclophosphamide and epirubicin to the cisplatin and etoposide combination produced a slight survival benefit, but at the expense of greater toxicity (Loehrer *et al*, 1995; Pujol *et al*, 2001). Phase III trials of cisplatin and etoposide with or without paclitaxel showed unacceptable toxicity with 6–13% toxic deaths in the paclitaxel-containing arm (Mavroudis *et al*, 2001; Niell *et al*, 2005). The results in these studies and the current study are consistent in the increased toxicity despite the G-CSF support and no definite survival benefit in the three or four drug combinations over the standard doublet in patients with ED-SCLC.

In conclusion, the IPE regimen was marginally more effective than the IP regimen, but was too toxic despite the administration of prophylactic G-CSF.

ACKNOWLEDGEMENTS

This study was supported, in part, by Grants-in-Aid for Cancer Research from the Ministry of Health, Labour and Welfare of Japan. We thank the following doctors for their care for patients and valuable suggestion and comments on this study: Takahiko Sugiura, Aichi Cancer Center; Yoshinobu Ohsaki, Asahikawa Medical College; Shinzo Kudoh, Osaka City University Medical School; Makoto Nishio, Cancer Institute Hospital; Hiroshi Chiba, Kumamoto Community Medical Center; Koichi Minato, Gunma Prefectural Cancer Center; Naoyuki Nogami, Shikoku Cancer Center; Hiroshi Ariyoshi, Aichi Cancer Center Aichi Hospital; Takamune Sugiura, Rinku General Medical Center; Akira Yokoyama, Niigata Cancer Center Hospital; and Koshiro Watanabe, Yokohama Municipal Citizen's Hospital. We also thank Fumiko Koh, Yuko Yabe and Mika Nagai for preparation of the paper.

REFERENCES

Armitage P, Berry G, Matthews J (2002) Survival analysis. In *Statistical Methods in Medical Research*, Armitage P, Berry G, Matthews J (eds), pp 568–590. Oxford: Blackwell Science Ltd

Fukuoka M, Furuse K, Saijo N, Nishiwaki Y, Ikegami H, Tamura T, Shimoyama M, Suemasu K (1991) Randomized trial of cyclophosphamide, doxorubicin, and vincristine *vs* cisplatin and etoposide *vs* alternation of these regimens in small-cell lung cancer. *J Natl Cancer Inst* **83**: 855–861

Hanna N, Bunn Jr PA, Langer C, Einhorn L, Guthrie Jr T, Beck T, Ansari R, Ellis P, Byrne M, Morrison M, Hariharan S, Wang B, Sandler A (2006) Randomized phase III trial comparing irinotecan/cisplatin with etoposide/cisplatin in patients with previously untreated extensive-stage disease small-cell lung cancer. *J Clin Oncol* **24**: 2038–2043

Hryniuk WM, Goodyear M (1990) The calculation of received dose intensity. *J Clin Oncol* **8**: 1935–1937

Jackman DM, Johnson BE (2005) Small-cell lung cancer. *Lancet* **366**: 1385–1396

Liu PY, Dahlberg S, Crowley J (1993) Selection designs for pilot studies based on survival. *Biometrics* **49**: 391–398

Loehrer Sr PJ, Ansari R, Gonin R, Monaco F, Fisher W, Sandler A, Einhorn LH (1995) Cisplatin plus etoposide with and without ifosfamide in extensive small-cell lung cancer: a Hoosier Oncology Group study. *J Clin Oncol* **13**: 2594–2599

Mavroudis D, Papadakis E, Veslemes M, Tsiafaki X, Stavrakakis J, Kouroussis C, Kakolyris S, Bania E, Jordanoglou J, Agelidou M, Vlachonicolis J, Georgoulias V (2001) A multicenter randomized clinical trial comparing paclitaxel–cisplatin–etoposide *vs* cisplatin–etoposide as first-line treatment in patients with small-cell lung cancer. *Ann Oncol* **12**: 463–470

Niell HB, Herndon II JE, Miller AA, Watson DM, Sandler AB, Kelly K, Marks RS, Perry MC, Ansari RH, Otterson G, Ellerton J, Vokes EE, Green MR (2005) Randomized phase III intergroup trial of etoposide and cisplatin with or without paclitaxel and granulocyte colony-stimulating factor in patients with extensive-stage small-cell lung cancer: Cancer and Leukemia Group B Trial 9732. *J Clin Oncol* **23**: 3752–3759

Noda K, Nishiwaki Y, Kawahara M, Negoro S, Sugiura T, Yokoyama A, Fukuoka M, Mori K, Watanabe K, Tamura T, Yamamoto S, Saijo N (2002) Irinotecan plus cisplatin compared with etoposide plus cisplatin for extensive small-cell lung cancer. *N Engl J Med* **346**: 85–91

Pujol JL, Daures JP, Riviere A, Quoix E, Westeel V, Quantin X, Breton JL, Lemarie E, Poudenx M, Milleron B, Moro D, Debieuvre D, Le Chevalier T (2001) Etoposide plus cisplatin with or without the combination of 4′-epidoxorubicin plus cyclophosphamide in treatment of extensive small-cell lung cancer: a French Federation of Cancer Institutes multicenter phase III randomized study. *J Natl Cancer Inst* **93**: 300–308

Roth BJ, Johnson DH, Einhorn LH, Schacter LP, Cherng NC, Cohen HJ, Crawford J, Randolph JA, Goodlow JL, Broun GO, Omura GA, Greco FA (1992) Randomized study of cyclophosphamide, doxorubicin, and vincristine *vs* etoposide and cisplatin *vs* alternation of these two regimens in extensive small-cell lung cancer: a phase III trial of the Southeastern Cancer Study Group. *J Clin Oncol* **10**: 282–291

Sekine I, Nishiwaki Y, Noda K, Kudoh S, Fukuoka M, Mori K, Negoro S, Yokoyama A, Matsui K, Ohsaki Y, Nakano T, Saijo N (2003) Randomized phase II study of cisplatin, irinotecan and etoposide combinations administered weekly or every 4 weeks for extensive small-cell lung cancer (JCOG9902-DI). *Ann Oncol* **14**: 709–714

Therasse P, Arbuck SG, Eisenhauer EA, Wanders J, Kaplan RS, Rubinstein L, Verweij J, Van Glabbeke M, van Oosterom AT, Christian MC, Gwyther SG (2000) New guidelines to evaluate the response to treatment in solid tumors. European Organization for Research and Treatment of Cancer, National Cancer Institute of the United States, National Cancer Institute of Canada. *J Natl Cancer Inst* **92**: 205–216

Drug Metab. Pharmacokinet. 22 (6): *SNP56* (462)-*SNP61* (467) (2007).

SNP Communication

Genetic Variations of VDR/NR1I1 Encoding Vitamin D Receptor in a Japanese Population

Maho UKAJI[1], Yoshiro SAITO[1,2,*], Hiromi FUKUSHIMA-UESAKA[1], Keiko MAEKAWA[1,2], Noriko KATORI[1,3], Nahoko KANIWA[1,4], Teruhiko YOSHIDA[5], Hiroshi NOKIHARA[6], Ikuo SEKINE[6], Hideo KUNITOH[6], Yuichiro OHE[6], Noboru YAMAMOTO[6], Tomohide TAMURA[6], Nagahiro SAIJO[7] and Jun-ichi SAWADA[1,2]

[1]*Project Team for Pharmacogenetics,* [2]*Division of Biochemistry and Immunochemistry,* [3]*Division of Drugs,* [4]*Division of Medicinal Safety Science, National Institute of Health Sciences, Tokyo, Japan* [5]*Genomics Division, National Cancer Center Research Institute,* [6]*Thoracic Oncology Division, National Cancer Center Hospital, National Cancer Center, Tokyo, Japan* [7]*Deputy Director, National Cancer Center Hospital East, National Cancer Center, Chiba, Japan*

Full text of this paper is available at http://www.jstage.jst.go.jp/browse/dmpk

Summary: The vitamin D receptor (VDR) is a transcriptional factor responsive to 1α,25-dihydroxyvitamin D_3 and lithocholic acid, and induces expression of drug metabolizing enzymes CYP3A4, CYP2B6 and CYP2C9. In this study, the promoter regions, 14 exons (including 6 exon 1's) and their flanking introns of *VDR* were comprehensively screened for genetic variations in 107 Japanese subjects. Sixty-one genetic variations including 25 novel ones were found: 9 in the 5′-flanking region, 2 in the 5′-untranslated region (UTR), 7 in the coding exons (5 synonymous and 2 nonsynonymous variations), 12 in the 3′-UTR, 19 in the introns between the exon 1's, and 12 in introns 2 to 8. Of these, one novel nonsynonymous variation, 154A>G (Met52Val), was detected with an allele frequency of 0.005. The single nucleotide polymorphisms (SNPs) that increase VDR expression or activity, -29649G>A, 2T>C and 1592(*308)C>A tagging linked variations in the 3′-UTR, were detected at 0.430, 0.636, and 0.318 allele frequencies, respectively. Another SNP, -26930A>G, with reduced *VDR* transcription was found at a 0.028 frequency. These findings would be useful for association studies on *VDR* variations in Japanese.

Key words: *VDR*; SNPs; nonsynonymous variation; Japanese

Introduction

The vitamin D receptor (VDR) is a nuclear receptor, which acts as a transcriptional factor upon binding of the active form of vitamin D, 1α,25-dihydroxyvitamin D_3 [1,25$(OH)_2D_3$], and lithocholic acid.[1-3] Ligand-activated VDR forms a heterodimer with retinoid X receptor, binds to the vitamin D responsive-element and induces expression of its target genes, resulting in partial arrest in G_0/G_1 of the cell cycle, induction of differentiation, or control of calcium homeostatis and maintenance of bone. In addition, VDR has been shown to be involved in induction of drug metabolizing enzymes CYP3A4, CYP2B6 and CYP2C9 in human primary hepatocytes,[2,4] and CYP3A4 in intestinal cell lines.[2,5] VDR and pregnane X receptor share 63% amino acid sequence identity in their DNA binding domains.[2] Like pregnane X receptor and constitutive androstane receptor, VDR transactivates *CYP3A4* through binding to its distal DR3 and proximal ER6 elements.[4,5] Recently, CYP3A4 has been shown to catalyze hydroxylation of

As of August 16, 2007, the novel variations reported here are not found in the database of Japanese Single Nucleotide Polymorphisms (http://snp.ims.u-tokyo.ac.jp/), dbSNP in the National Center for Biotechnology Information (http://www.ncbi.nlm.nih.gov/SNP/), or PharmGKB Database (http://www.pharmgkb.org/).

This study was supported in part by the Program for the Promotion of Fundamental Studies in Health Sciences from National Institute of Biomedical Innovation and the Health and Labor Sciences Research Grants from the Ministry of Health, Labor and Welfare.

Received; August 17, 2007, Accepted September 21, 2007

**To whom correspondence should be addressed*: Yoshiro SAITO, Ph.D., *Division of Biochemistry and Immunochemistry, National Institute of Health Sciences, 1-18-1 Kamiyoga, Setagaya-ku, Tokyo 158-8501, Japan. Tel. +81-3-5717-3831, Fax. +81-3-5717-3832, E-mail: yoshiro@nihs.go.jp*

$1,25(OH)_2D_3$ in human liver and intestine, suggesting negative feedback control of $1,25(OH)_2D_3$ action.[6]

The *VDR* gene consists of 6 exon 1's (exons 1f, 1e, 1a, 1d, 1b, and 1c in this order) and 8 other exons (exons 2 to 9), and spans approximately 100 kb at chromosome 12q13.11.[7] The VDR protein is expressed in many tissues including kidney, skin and liver.[1] Alternative usage of exon 1's yields 14 transcripts including 3 major types: exon 1a-1c, exon 1d-1c or exon 1f-1c combinations, followed by common exons 2-9.[7] A translational initiation codon in exon 2 is used in transcripts starting from exon 1a or 1f. In the transcript from exon 1d (1d transcript), translation could initiate from the ATG codon in exon 1d, generating an active protein 50 amino acids longer than that from the exon 1a- or 1f-containing transcript (1a or 1f transcript).[7,8] However, the 1d and 1f transcripts are assumed to be minor (expression levels were less than 10 and 20%, respectively, of the 1a transcript).[7]

Genetic polymorphisms of transcriptional factors involved in induction of drug metabolizing enzymes could influence their expression levels, and as a result drug pharmacokinetics/pharmacodynamics. As for *VDR*, several polymorphisms with functional significance have been reported.[9] For example, the single nucleotide polymorphism (SNP) 2T>C (*Fok*I polymorphism) in the first ATG codon of 1a and 1f transcripts results in generation of a three amino acid shorter protein, which has a significantly higher transcriptional activity than the longer transcript.[9,10] Another SNP -29649G>A upstream of exon 1e (thus exons 1a and 1d) is located in the Cdx2 (an intestinal transcriptional factor)-binding element. This nucleotide change facilitates Cdx2 binding, resulting in increased *VDR* transcription.[9,11]

Recently, Nejentsev *et al.* resequenced *VDR* and found 245 genetic variations in Caucasians (Britons).[12] However, no comprehensive screening of *VDR* polymorphisms has been reported for Asian populations including Japanese. In this study, we searched for *VDR* variations by resequencing the promoter regions, all 14 exons and their surrounding introns from 107 Japanese subjects.

Materials and Methods

Human genomic DNA samples: One hundred and seven Japanese cancer patients administered paclitaxel were analyzed. Written informed consent was obtained from all subjects. The ethical review boards of the National Cancer Center and the National Institute of Health Sciences approved this study. DNA was extracted from whole blood, which was collected from the patients prior to paclitaxel administration.

DNA sequencing

Amplification of exon 1's, and exons 2 to 6: First, three sets of PCRs were separately performed to amplify exons 1f to 1b (Mix 1 primer set), the Cdx2 region (Mix 2), and exons 1c to 6 (Mix 3) from 50 ng of genomic DNA using 1.25 units of Z-Taq (Takara Bio Inc., Shiga, Japan) with 2 μM of each primer designed in the intronic regions (**Table 1**, 1st PCR). The first PCR conditions were 30 cycles of 98°C for 5 sec, 55°C for 5 sec, and 72°C for 190 sec. Next, exon 1's and exon 2 with high GC content were amplified separately from the 1st PCR product as a template with 2.5 units of LA-Taq (Takara Bio Inc.) in GC buffer I and 1 μM of each primer (2nd PCR in **Table 1**). For the Cdx2 region and exons 3 to 6, PCR reactions were performed using Ex-Taq (1 unit, Takara Bio Inc.) and 0.4 μM of primers in **Table 1**. The second PCR conditions were 94°C for 5 min, followed by 30 cycles of 94°C for 30 sec, 60°C for 1 min, and 72°C for 2 min, and then a final extension for 7 min at 72°C.

Amplification of exons 7 to 9: These exons were directly amplified from 50 ng DNA. Amplification was performed with Ex-Taq for exons 7 to 8, 9-1 and 9-3, and with LA-Taq in GC buffer I for exon 9-2. Primer concentrations, polymerase units and PCR conditions were the same as described above for the second round PCR.

Sequencing: PCR products were treated with a PCR Product Pre-Sequencing Kit (USB Co., Cleveland, OH, USA) and directly sequenced on both strands using an ABI BigDye Terminator Cycle Sequencing Kit ver. 3.1 (Applied Biosystems, Foster City, CA, USA) with sequencing primers listed in **Table 1** (Sequencing). Excess dye was removed by a DyeEx96 kit (Qiagen, Hilden, Germany) and the eluates were analyzed on an ABI Prism 3730 DNA Analyzer (Applied Biosystems). All novel SNPs were verified by sequencing PCR products obtained by a new genomic DNA amplification. Under the conditions used, up to 1,640 bases upstream of exon 1f, up to 4,090 (4,460) bases upstream of exon 1a (1d), all exons and their flanking introns were successfully sequenced for all subjects. *VDR* genomic sequence (NT_029419.11) and cDNA sequence (exon 1a-1c transcript, NM_000376.2) obtained from GenBank were used as reference sequences. Nucleotide positions based on cDNA sequence were numbered from the adenine of the translational start site (10416202 in NT_029419.11 and 161 in NM_000376.2) or the nearest exons (for introns 2 to 8).

Other analysis: Hardy-Weinberg equilibrium and linkage disequilibrium (LD) analyses were performed with SNPAlyze version 3.1 (Dynacom Co., Yokohama, Japan), and pairwise LDs between variations were obtained for rho square (r^2) values. P-values for Hardy-Weinberg equilibrium were corrected by false-discovery

Table 1. Primers used for sequencing *VDR*

		Amplified or sequensed region	Forward primer (5′ to 3′)	Reverse primer (5′ to 3′)	Amplified length (bp)
1st PCR	Mix 1	Exon 1f	TTGTTGACTCTCCTGGCTTTATCAG	CCAGTCACTTTGAAGAGAAACCTGC	3,823
		Exon 1e, 1a, 1d, 1b	TGGTCCCTTCTGTCTTTCTAACTCC	TTGGGAGGATGTAGAACCGTGGGAT	10,421
	Mix 2	Cdx2	ACTGGTGGTGCCCTACTCTTTCT	TTGGGAGGATGTAGAACCGTGGGAT	11,835
	Mix 3	Exon 1c to Exon 2	GCTAAAAGTGGCAGAAAACATCCTG	TTGTGTTGACAGAGAGACCCCAAGT	5,476
		Exon 3	TAGCATCCTTACTTCTCATAGCGGC	CCTGTTCTGTGACTTATCCTCTGTC	2,556
		Exons 4 to 6	TGGTGTGGCTGGCAGAAACAGGTCT	TCTCTCAAAGTGTTGGGATAGGCAT	4,847
		Exons 7 to 8	AACACTCTTGTCCCTTCCAG	TCTGTGTCTCCTTTTGCTAC	753
		Exon 9-1	GTCAGCAGTCATAGAGGGGT	CAGATGGAGAAGATGCGGCT	1,327
		Exon 9-2	AGAGGGTCTGGAGAAGCAGT	AATGAGGGGATTGACTCGTT	1,012
		Exon 9-3	TCTTCAGTGGGAGAAAACAC	CTGTCAAATGGGGGTAATAA	1,417
2nd PCT		Exon 1f	GAACCCTTTTCTCTGCCCTCACCTT	AGACAGAGGACTGGAGAAGGAGATA	606
			ACTCTGCTCCTTCACCACCTCTACA	AAACTGAGTGCGTGTGAGTGAGAGA	628
			GCTGGAGGTGTTGAACTGGTTGCTT	CGCATACCCGACACTTGTTCACCTC	851
		Cdx 2	GTAATCCTTCCACCTCAACTTCCTA	CCACAGAGTCCAAAGAAAGGCAGGG	1,148
		Exon 1e	AGAGGAGAGGGTCTGGAGAG	TTCCAACCACCAATACCTTG	640
		Exon 1e to 1a	GCAGAGAATGTCCCAAGGTA	GACCGTCGTCCATAGGGCAA	1,411
		Exon 1a to 1d	AGAAGCGTGCCTTGCCCTAT	CTGAACATCTATTGACAGGC	871
		Exon 1b	CTGGAAGGCAAATAGGAAAC	GCCGTGTAAAGCAGTGGTTA	368
		Exon 1c	GCTGTGAGAGGAGAAGGAGT	GCAAAATCCTGGGTGGTATC	517
		Exon 2	GTGAACCACTAAACCCAAAT	GAAGGAGATGTGAAAAATGC	528
		Exon 3	TCTGTTGGAGAAATGGAGAC	GCCTCTGACACCAACACACA	478
		Exons 4 to 5	TGCCTTCCTTTTCACCATAG	AGAGGGGCTGTTGTGAAGAC	912
		Exon 6	TGAAAGAGGCAGAGAGAGTC	GGTTATAGTGAGCCAAGATAGTG	719
Sequencing		Exon 1f	GAACCCTTTTCTCTGCCCTCACCTT	AGACAGAGGACTGGAGAAGGAGATA	
			ACTCTGCTCCTTCACCACCTCTACA	AAACTGAGTGCGTGTGAGTGAGAGA	
			GCTGGAGGTGTTGAACTGGTTGCTT	CAGGACAGCAGGACCTTCAGGGAAC	
			CACTGACTCTCACCTTCCTTTCCTC	CGCATACCCGACACTTGTTCACCTC	
			GGTGGCTCCCTCCTGCTGTGTGG		
		Cdx2	AGGAAGGAAGGAAAAGAGGAT	TGGAGTTAGAAAGACAGAAGGGACC	
		Exon 1e	TGTTTTTTAGAGGCAGCAT	TTCCAACCACCAATACCTTG	
			TAGAGGCAGCATGAAACAGT	GATGGATGGATTCTCTACCT	
		Exon 1e to 1a	GCAGAGAATGTCCCAAGGTA	CTCACAAAATCATCCAGCAG	
			CTGGCTAAAGGAGGTCATCG	CGCTCGCCAACCTGTTACTG	
			CAGTAACAGGTTGGCGAGCG	GACCGTCGTCCATAGGGCAA	
			CGACTGCTGGATGATTTTGT	CGATGATTATAGGTGCGGAT	
		Exon 1a	AGCGTGCCTTGCCCTATGGA	TTTACCGCTGAGACTTAGAC	
		ERxon 1d	AAACTTGGCTACTGAGGTCC	TAAAAGACCCAACTCCACC	
		Exon 1b	CTGGAAGGCAAATAGGAAAC	GCCGTGTAAAGCAGTGGTTA	
		Exon 1c	CTTCCCACTGCTCCTGCTAC	GGTGGTATCCCTTCCTTCCC	
		Exon 2	GTGAACCACTAAACCCAAAT	GAAGGAGATGTGAAAAATGC	
		Exon 3	TCTGTTGGAGAAATGGAGAC	GCCTCTGACACCAACACACA	
		Exon 4	TGCCTTCCTTTTCACCATAG	CGTCCCTACCCCAGTTCTGT	
		Exon 5	ACAGAACTGGGGTAGGGACG	AGAGGGGCTGTTGTGAAGAC	
		Exon 6	TGAAAGAGGCAGAGAGAGTC,	GAAGTTTCTTACCTGAATCCTGG	
		Exon 6	CACTCATCCACCACTTCTTT	TGGTGTCTGGTGCCTGTAATCCC	
		Exons 7 to 8	AACACTCTTGTCCCTTCCAG	TCTGTGTCTCCTTTTGCTAC	
		Exon 9-1	GGTGCTGCCGTTGAGTGTCT	ACATCAGTCAGCAGCCACTT	
			AAGTGGCTGCTGACTGATGT	GAAGATGCGGCTCACTGCTT	
		Exon 9-2	AGCCGCATCTTCTCCATCTG	GCCGCATTCCCCAAACTCAA	
			TTGAGTTTGGGGAATGCGGC	AATGAGGGGATTGACTCGTT	
		Exon 9-3	TCTTCAGTGGGAGAAAACAC	ATGTTGGTCAGGTTGGTCTC	
			GGAGGCTGAGGCAGAAGAAT	CCAGGGCTGAGTAACTGATA	
			CCTGCCTTCTTCGGGGAACT	CTGTCAAATGGGGGTAATAA	

Table 2. Summary of *VDR* variations detected in this study

SNP ID		Location	Position		Nucleotide change	Amino acid change	Allele frequency (n=214)
This Study	dbSNP (NCBI)		NT_029419.11	From the translational start site[d] or from the end of the nearest exon			
MPJ6_VDR_001	rs4547172	5′-flanking	10481728	-65526	tccatatttatcT/Cttttatacttct		0.238
MPJ6_VDR_002	rs4583039	5′-flanking	10481720	-65518	tatccttttataC/Tttctttcaagt		0.252
MPJ6_VDR_003	rs7970376	5′-flanking	10481502	-65300	cattaaacagatG/Atatcatcatctg		0.037
MPJ6_VDR_004	rs4237856	5′-flanking	10481356	-65154	cccaggctcagcT/Ggccctttgacat		0.196
MPJ6_VDR_005[a]		5′-flanking	10480937	-64735	tgtgccaggtagG/Ccgtggtgccccc		0.028
MPJ6_VDR_006	rs3923693	5′-flanking	10480935	-64733	tgccaggtaggcG/Atggtgcccccgc		0.327
MPJ6_VDR_007	rs4073726	5′-flanking	10480623	-64421	cgtcctccctggG/Ccaagccatctcc		0.037
MPJ6_VDR_008[a]		5′-flanking	10480382	-64180	cttctggtgcccC/Gcctgctccctca		0.061
MPJ6_VDR_009	rs4073729	5′-flanking	10480375	-64173	tgccccccctgctC/Tctcatggccag		0.229
MPJ6_VDR_010	rs11168297	inton 1f-1e[b]	10446202	-30000	gtactgggattaC/Taggcctgagcca		0.028
MPJ6_VDR_011	rs17880972	inton 1f-1e[b]	10446166	-29964	aggatttttaatA/Gtgtattttggg		0.028
MPJ6_VDR_012	rs11568820	inton 1f-1e[b]	10445851	-29649 (Cdx2)	aactaggtcacaG/Ataaaaacttatt		0.430
MPJ6_VDR_013[a]		inton 1f-1e[b]	10445734	-29532	cattctatttttA/Gccatctggaaca		0.005
MPJ6_VDR_014[a]		inton 1f-1e[b]	10445338	-29136	catggggacaggG/Atctctgggagac		0.005
MPJ6_VDR_015	rs11614332	inton 1f-1e[b]	10445204	-29002	gatgaggacaggC/Ttgcagtcctgtg		0.028
MPJ6_VDR_016[a]		inton 1e-1a[b]	10443873	-27671	aacaaaggctgtG/Aaaaaaagactaa		0.028
MPJ6_VDR_017[a]		inton 1e-1a[b]	10443771	-27569	gtcaagcaccacA/Taaagtgacttct		0.028
MPJ6_VDR_018	rs7139166	inton 1e-1a[b]	10443640	-27438	tagctttcccacG/Catgctttgggca		0.028
MPJ6_VDR_019[a]		inton 1e-1a[b]	10443419	-27217	cagtgcttaacaA/Gacttcactgttg		0.005
MPJ6_VDR_020	rs4516035	inton 1e-1a[b]	10443132	-26930 (GATA)	gcgaatagcaatA/Gtcttccctggct		0.028
MPJ6_VDR_021	rs11574006	inton 1e-1a[b]	10442825	-26623	tgccacggggcgG/Tgggggaaggcg		0.023
MPJ6_VDR_022	rs11574007	inton 1e-1a[b]	10442819_10442818	-26617_-26616	gggcgggggggg/insG/aaggcggaactc		0.014
MPJ6_VDR_023	rs11574007	inton 1e-1a[b]	10442819_10442818	-26617_-26616	gggcgggggggg/insGG/aaggcggaactc		0.023
MPJ6_VDR_024[a]		inton 1e-1a[b]	10442795	-26593	cgggaccagggaC/Tcagggaagctga		0.028
MPJ6_VDR_025[a]		inton 1e-1a[b]	10442587	-26385	tggcgagcggagC/Tccgggatttccc		0.028
MPJ6_VDR_026[a]		inton 1e-1a[b]	10442542	-26340	cggtgccagtcgG/Tcaggcgcccccc		0.023
MPJ6_VDR_027	rs11574012	inton 1d-1b[b]	10441601	-25399	ggtcacctgtgaT/Cggtggagttggg		0.093
MPJ6_VDR_028	rs11168293	exon 1b (5′-UTR)	10437022	-20820	agcccagctggaC/Aggagaaatggac		0.028
MPJ6_VDR_029[a]		exon 1b (5′-UTR)	10436972	-20770	ccaggccccgtgC/Tacattgctttgc		0.014
MPJ6_VDR_030	rs11168292	inton 1b-1c[b]	10436911	-20709	aagtacagttatG/Cttctctagcagg		0.028
MPJ6_VDR_031	rs10735810	exon 2	10416201	2 (*Fok*I)	ttcttacagggaT/Cggaggcaatggc	Translational start site change	0.636
MPJ6_VDR_032	rs10783218	intron 2	10416049	IVS2+8	ttcaggtgagccC/Ttcctcccaggct		0.065
MPJ6_VDR_033[a]		intron 2	10415986	IVS2+71	tccatgaagggaG/Acccttgcatttt		0.005
MPJ6_VDR_034[a]		exon 3	10402259	154	ggcaggcgaagcA/Gtgaagcggaagg	Met52Val	0.005
MPJ6_VDR_035	rs11168267	intron 3	10394848	IVS3-71	ggacctttacccC/Tcaaccgcaggag		0.151
MPJ6_VDR_036	rs11168266	intron 3	10394839	IVS3-62	cccccaaccgcaG/Agaggaaggtttc		0.360
MPJ6_VDR_037[a]		intron 3	10394802	IVS3-25	ctggccagccctC/Tctgactcccctt		0.005
MPJ6_VDR_038[a]		intron 4	10394565	IVS4+28	gggaggatgagcC/Tggtccagaggag		0.014
MPJ6_VDR_039[a]		exon 5	10394225	576	tcactgtatcacC/Ttcttcaggtaag	Thr192Thr	0.005
MPJ6_VDR_040[a]		intron 6	10392586	IVS6+133	cttgctctgtcaC/Tgcaggctggagt		0.014
MPJ6_VDR_041	rs11168265	intron 6	10392565	IVS6+154	gagtgcagtggcG/Acgatctcggctc		0.150
MPJ6_VDR_042	rs11574093	intron 6	10392429_10392428	IVS6+290_291	atttatttattt/insATTT/ttatttttttc		0.187
MPJ6_VDR_043[a]		exon 7	10383807	846	cttcaccatggaC/Tgacatgtcctgg	Asp282Asp	0.005
MPJ6_VDR_044	rs11574113	intron 8	10382206	IVS8-112	catagaggggtgG/Ccctaggggtgc		0.154
MPJ6_VDR_045[a]		intron 8	10382176	IVS8-82	ttgagtgtctgtG/Atgggtgggggt		0.047
MPJ6_VDR_046	rs7975232	intron 8	10382143	IVS8-49 (*Apa*I)	tgagcagtgaggG/Tgcccagctgaga		0.318
MPJ6_VDR_047	rs731236	exon 9	10382063	1056 (*Taq*I)	cgccgcgctgatT/Cgaggccatccag	Ile352Ile	0.164
MPJ6_VDR_048[a]		exon 9	10381988	1131	cccgggcagccaC/Tctgctctatgcc	His377His	0.005
MPJ6_VDR_049	rs2229829	exon 9	10381913	1206′	caagcagtaccgC/Atgcctctcctte	Arg402Arg	0.014
MPJ6_VDR_050	rs739837	3′-UTR	10381527	1592 (*308)[c]	ctccaccgctgcC/Ataagtggctgct		0.318
MPJ6_VDR_051	rs3847987	3′-UTR	10381374	1745(*461)[c]	gataaataatcgG/Tcccacagctccc		0.154
MPJ6_VDR_052[a]		3′-UTR	10381348	1771 (*487)[c]	ccccacccccttC/Tagtgcccaccaa		0.005
MPJ6_VDR_053[a]		3′-UTR	10381047	2072 (*788)[c]	cgacctcgtcctC/Acccctgccagtg		0.005
MPJ6_VDR_054	rs11574125	3′-UTR	10381042	2077 (*793)[c]	tcgtcctccccc/delT/gccagtgcctta		0.318
MPJ6_VDR_055[a]		3′-UTR	10380870	2249 (*965)[c]	gaagaattttcaG/Caccccagcggct		0.005
MPJ6_VDR_056	rs11574129	3′-UTR	10380609	2510 (*1226)[c]	tcaagtgcatgcT/Cctctgcagccag		0.126
MPJ6_VDR_057	rs11574131	3′-UTR	10380516	2603 (*1319)[c]	aggtgtgcgggaC/Tcggtacagaaag		0.042
MPJ6_VDR_058	rs9729	3′-UTR	10379929	3190 (*1906)[c]	aatcccctcattC/Aaggaaaactgac		0.322
MPJ6_VDR_059[a]		3′-UTR	10379840	3279 (*1995)[c]	gcggtggctcacG/Acctgtaatccca		0.005
MPJ6_VDR_060	rs2853562	3′-UTR	10379692	3427 (*2143)[c]	catggtggcgcaA/Tgcctgtaatccc		0.322
MPJ6_VDR_061[a]		3′-UTR	10379608	3511 (*2227)[c]	tgagatcgtgccG/Attactctccaac		0.037

[a]Novel variations detected in this study.
[b]The intronic region between the two exon 1's indicated.
[c]The position with an asterisk in parenthesis is numbered from the translational termination codon TGA.
[d]The translational start site in exon 2 was used for numbering according to NM_000376.2.

rate methods.[13]

Results and Discussion

We found 61 genetic variations, including 25 novel ones, from 107 Japanese subjects (**Table 2**). Of them, 9 were located in the 5′-flanking region of exon 1f, 19 in the introns between the exon 1's, 2 in the 5′-untranslated region (UTR), 7 in the coding exons (5 synonymous and 2 nonsynonymous variations), 12 in the 3′-UTR, and 12 in introns 2 to 8. All observed allele frequencies were in Hardy-Weinberg equilibrium ($p > 0.05$) after correction for multiple comparison, except for 3 linked variations -27671G>A, -26593C>T and -26385C>T. Deviations from equilibrium were derived from an unexpected occurrence of one minor allele homozygote in these low frequency variations. However, the occurrence at these positions was confirmed by repeated sequencing.

One novel nonsynonymous variation, 154A>G (Met52Val), was found heterozygously with an allele frequency of 0.005. The Met52Val is found in the nuclear localization signal between two zinc finger regions.[14] Furthermore, the precedent amino acid Ser51 is phosphorylated by protein kinase C, which could modulate the VDR binding to the vitamin D responsive-element and transactivation activity.[15] Thus, functional significance of this Met52Val variation should be clarified in future studies.

One known nonsynonymous SNP, 2T>C (the *Fok*I polymorphism) that results in increased transcriptional activity, was also detected at a 0.636 allele frequency, which is similar to frequencies reported for Japanese women (0.59)[10] and Caucasians (0.62),[16] but slightly higher than that in Chinese (0.53)[17] and lower than that in African-Americans (0.79).[16]

Other functionally relevant SNPs are -29649G>A and -26930A>G. The SNP -29649G>A, leading to higher affinity for Cdx2 and increased *VDR* transcription, was detected at a 0.430 frequency, which is higher and lower than those in Caucasians (0.17) and Africans (0.75), respectively.[18] By luciferase reporter and electrophoretic mobility shift assays, the other SNP -26930A>G was shown to two-fold reduce *VDR* transcription with decreased binding affinity to a GATA protein.[18] The allele frequency of this variation was 0.028, which is comparable to that in Africans (0.06) but considerably lower than that in Caucasians (0.43).[18] Since GATA family proteins are expressed in many tissues,[19] this variation might be important for interindividual differences in VDR expression levels.

Fang *et al.* (2005) reported that the 3′-UTR SNPs 1592(*308)C>A, 2077(*793)delT, 3190(*1906)C>A, 3387(*2103)_3406(*2122)$A_{20}>A_{13\text{-}24}$ and 3427(*2143)A>T were in high LD in Caucasians, and that the major haplotype 1592(*308)C-2077(*793)T-3190(*1906)C-3387(*2103)_3406(*2122)A_{22}-3427(*2143)A showed a 15% lower level and 30% faster decay of VDR mRNA than the minor reciprocal haplotype.[18] However, the variation responsible for these functional alterations has not been identified. In our hands, the polymorphism 3387(*2103)_3406(*2122)$A_{20}>A_{13\text{-}24}$ could not be precisely genotyped by direct sequencing and thus is not listed in **Table 2.** However, the four other SNPs were in very high LD ($r^2 \geq 0.979$) also in our Japanese population. Note that IVS8-49G>T (known as the *Apa*I polymorphism)[9] also linked to these four variations ($r^2 \geq 0.979$). Thus, VDR mRNA stability is probably influenced by this haplotype also in Japanese. The tagging SNP 1592(*308)C>A (or IVS8-49G>T) was detected at a 0.318 frequency, which is lower than that in Caucasians (0.55).[18] Moreover, it was shown that this SNP was also closely linked to IVS8+283G>A (the *Bsm*I polymorphism).[18]

In conclusion, we identified 61 genetic variations, including 25 novel ones, from 107 Japanese subjects in *VDR*. One novel variation results in an amino acid substitution. Close associations of 5 SNPs [(IVS8-49G>T, 1592 (*308) C>A, 2077 (*793) delT, 3190 (*1906)C>A, and 3427(*2143)A>T] were also shown in Japanese. This information would be useful for pharmacogenetic studies to investigate the associations of *VDR* variations with interindividual differences in drug metabolism catalyzed by VDR-regulated drug metabolizing enzymes in Japanese.

Acknowledgments: We thank Ms. Chie Sudo for her secretarial assistance. Authors Maho Ukaji and Yoshiro Saito contributed equally to this work.

References

1) Malloy, P. J., Pike, J. W. and Feldman, D.: The vitamin D receptor and the syndrome of hereditary 1,25-dihydroxyvitamin D-resistant rickets. *Endocr. Rev.*, **20**: 156–188 (1999).
2) Pascussi, J. M., Gerbal-Chaloin, S., Drocourt, L., Maurel, P. and Vilarem, M. J.: The expression of CYP2B6, CYP2C9 and CYP3A4 genes: a tangle of networks of nuclear and steroid receptors. *Biochim. Biophys. Acta.*, **1619**: 243–253 (2003).
3) Makishima, M., Lu, T. T., Xie, W., Whitfield, G. K., Domoto, H., Evans, R. M., Haussler, M. R. and Mangelsdorf, D. J.: Vitamin D receptor as an intestinal bile acid sensor. *Science*, **296**: 1313–1316 (2002).
4) Drocourt, L., Ourlin, J. C., Pascussi, J. M., Maurel, P. and Vilarem, M. J.: Expression of *CYP3A4*, *CYP2B6*, and *CYP2C9* is regulated by the vitamin D receptor pathway in primary human hepatocytes. *J. Biol. Chem.*, **277**: 25125–25132 (2002).
5) Thompson, P. D., Jurutka, P. W., Whitfield, G. K., Myskowski, S. M., Eichhorst, K. R., Dominguez, C. E., Haussler, C. A. and Haussler, M. R.: Liganded VDR in-

duces CYP3A4 in small intestinal and colon cancer cells *via* DR3 and ER6 vitamin D responsive elements. *Biochem. Biophys. Res. Commun.*, **299**: 730–738 (2002).
6) Xu, Y., Hashizume, T., Shuhart, M. C., Davis, C. L., Nelson, W. L., Sakaki, T., Kalhorn, T. F., Watkins, P. B., Schuetz, E. G. and Thummel, K. E.: Intestinal and hepatic CYP3A4 catalyze hydroxylation of 1α,25-dihydroxyvitamin D_3: implications for drug-induced osteomalacia. *Mol. Pharmacol.*, **69**: 56–65 (2006).
7) Crofts, L. A., Hancock, M. S., Morrison, N. A. and Eisman, J. A.: Multiple promoters direct the tissue-specific expression of novel N-terminal variant human vitamin D receptor gene transcripts. *Proc. Natl. Acad. Sci. USA*, **95**: 10529–10534 (1998).
8) Sunn, K. L., Cock, T. A., Crofts, L. A., Eisman, J. A. and Gardiner, E. M.: Novel N-terminal variant of human VDR. *Mol. Endocrinol.*, **15**: 1599–1609 (2001).
9) Uitterlinden, A. G., Fang, Y., Van Meurs, J. B., Pols, H. A. and Van Leeuwen, J. P.: Genetics and biology of vitamin D receptor polymorphisms. *Gene*, **338**: 143–156 (2004).
10) Arai, H., Miyamoto, K., Taketani, Y., Yamamoto, H., Iemori, Y., Morita, K., Tonai, T., Nishisho, T., Mori, S. and Takeda, E.: A vitamin D receptor gene polymorphism in the translation initiation codon: effect on protein activity and relation to bone mineral density in Japanese women. *J. Bone Miner. Res.*, **12**: 915–921 (1997).
11) Arai, H., Miyamoto, K., Yoshida, M., Yamamoto, H., Taketani, Y., Morita, K., Kubota, M., Yoshida, S., Ikeda, M., Watabe, F., Kanemasa, Y. and Takeda, E.: The polymorphism in the caudal-related homeodomain protein Cdx-2 binding element in the human vitamin D receptor gene. *J. Bone Miner. Res.*, **16**: 1256–1264 (2001).
12) Nejentsev, S., Godfrey, L., Snook, H., Rance, H., Nutland, S., Walker, N. M., Lam, A. C., Guja, C., Ionescu-Tirgoviste, C., Undlien, D. E., Ronningen, K. S., Tuomilehto-Wolf, E., Tuomilehto, J., Newport, M. J., Clayton, D. G. and Todd, J. A.: Comparative high-resolution analysis of linkage disequilibrium and tag single nucleotide polymorphisms between populations in the vitamin D receptor gene. *Hum. Mol. Genet.*, **13**: 1633–1639 (2004).
13) Benjamini, Y. and Hochberg, Y.: Controlling the false discovery rate: A practical and powerful approach to multiple testing. *J. Roy. Stat. Soc. B.*, **57**: 289–300 (1995).
14) Hsieh, J. C., Shimizu, Y., Minoshima, S., Shimizu, N., Haussler, C. A., Jurutka, P. W. and Haussler, M. R.: Novel nuclear localization signal between the two DNA-binding zinc fingers in the human vitamin D receptor. *J. Cell. Biochem.*, **70**: 94–109 (1998).
15) Hsieh, J. C., Jurutka, P. W., Nakajima, S., Galligan, M. A., Haussler, C. A., Shimizu, Y., Shimizu, N., Whitfield, G.K. and Haussler, M. R.: Phosphorylation of the human vitamin D receptor by protein kinase C. Biochemical and functional evaluation of the serine 51 recognition site. *J. Biol. Chem.*, **268**: 15118–15126 (1993).
16) Oakley-Girvan, I., Feldman, D., Eccleshall, T. R., Gallagher, R. P., Wu, A. H., Kolonel, L. N., Halpern, J., Balise, R. R., West, D. W., Paffenbarger, R. S. Jr. and Whittemore, A. S.: Risk of early-onset prostate cancer in relation to germ line polymorphisms of the vitamin D receptor. *Cancer Epidemiol. Biomarkers Prev.*, **13**: 1325–1330 (2004).
17) Wong, H .L., Seow, A., Arakawa, K., Lee, H. P., Yu, M. C. and Ingles, S. A.:Vitamin D receptor start codon polymorphism and colorectal cancer risk: effect modification by dietary calcium and fat in Singapore Chinese. *Carcinogenesis*, **24**: 1091–1095 (2003).
18) Fang, Y., van Meurs, J. B., d'Alesio, A., Jhamai, M., Zhao, H., Rivadeneira, F., Hofman, A., van Leeuwen, J. P., Jehan, F., Pols, H. A. and Uitterlinden, A. G.: Promoter and 3′-untranslated-region haplotypes in the vitamin D receptor gene predispose to osteoporotic fracture: The Rotterdam study. *Am. J. Hum. Genet.*, **77**: 807–823 (2005).
19) Viger, R. S., Taniguchi, H., Robert, N. M. and Tremblay, J. J.: Role of the GATA family of transcription factors in andrology. *J. Androl.*, **25**: 441–452 (2004).

Epidermal Growth Factor Receptor Mutation Detection Using High-Resolution Melting Analysis Predicts Outcomes in Patients with Advanced Non–Small Cell Lung Cancer Treated with Gefitinib

Toshimi Takano,[1,6] Yuichiro Ohe,[1] Koji Tsuta,[2] Tomoya Fukui,[1] Hiromi Sakamoto,[5] Teruhiko Yoshida,[5] Ukihide Tateishi,[3] Hiroshi Nokihara,[1] Noboru Yamamoto,[1] Ikuo Sekine,[1] Hideo Kunitoh,[1] Yoshihiro Matsuno,[2] Koh Furuta,[4] and Tomohide Tamura[1]

Abstract

Purpose: Epidermal growth factor receptor (*EGFR*) mutations, especially deletional mutations in exon 19 (DEL) and L858R, predict gefitinib sensitivity in patients with non–small cell lung cancer (NSCLC). In this study, we validated *EGFR* mutation detection using high-resolution melting analysis (HRMA) and evaluated the associations between *EGFR* mutations and clinical outcomes in advanced NSCLC patients treated with gefitinib on a larger scale.

Experimental Design: The presence of DEL or L858R was evaluated using HRMA and paraffin-embedded tissues and/or cytologic slides from 212 patients. In 66 patients, the results were compared with direct sequencing data.

Results: HRMA using formalin-fixed tissues had a 92% sensitivity and a 100% specificity. The analysis was successfully completed in 207 patients, and DEL or L858R mutations were detected in 85 (41%) patients. The response rate (78% versus 8%), time-to-progression (median, 9.2 versus 1.6 months), and overall survival (median, 21.7 versus 8.7 months) were significantly better in patients with *EGFR* mutations ($P < 0.001$). Even among the 34 patients with stable diseases, the time-to-progression was significantly longer in patients with *EGFR* mutations. Patients with DEL ($n = 49$) tended to have better outcomes than those with L858R ($n = 36$); the response rates were 86% and 67%, respectively ($P = 0.037$), and the median time-to-progression was 10.5 and 7.4 months, respectively ($P = 0.11$).

Conclusions: HRMA is a precise method for detecting DEL and L858R mutations and is useful for predicting clinical outcomes in patients with advanced NSCLC treated with gefitinib.

Gefitinib (Iressa; AstraZeneca) is an orally active, selective epidermal growth factor receptor (EGFR) tyrosine kinase inhibitor. Phase II studies have shown gefitinib antitumor activity in patients with advanced non–small cell lung cancer (NSCLC; refs. 1, 2). Several studies have shown that the response rate to gefitinib is higher in women, patients with adenocarcinoma, never smokers, and Japanese or East Asians (1–3); subsequently, somatic mutations in the kinase domain of *EGFR* were suggested to be a determinant of gefitinib sensitivity (4, 5). Since then, many retrospective studies have consistently revealed that *EGFR* mutations, mainly in-frame deletions including amino acids at codons 747 to 749 in exon 19 (DEL) and a missense mutation at codon 858 (L858R) in exon 21, are associated with tumor response, time-to-progression, and overall survival in NSCLC patients treated with gefitinib (6–8).

In our previous study, which clearly showed a correlation between *EGFR* mutations and gefitinib sensitivity in patients with recurrent NSCLC after surgical resection of the primary tumor (6), we used methanol-fixed, paraffin-embedded surgical specimens and did laser capture microdissection and direct sequencing, which we considered to be the most precise methods available for identifying mutations at that time. However, these methods are not useful in clinical practice for the treatment of advanced NSCLC for two reasons. First, the diagnostic samples of advanced NSCLC tumors, unlike surgical specimens, contain a small amount of tumor cells and are highly contaminated with normal cells. Second, laser capture microdissection and direct sequencing require special

Authors' Affiliations: [1]Division of Internal Medicine, [2]Clinical Laboratory Division, [3]Division of Diagnostic Radiology, and [4]Clinical Support Laboratory, National Cancer Center Hospital; [5]Genetics Division, National Cancer Center Research Institute; and [6]Division of Medical Oncology, Tokyo Kyosai Hospital, Tokyo, Japan
Received 3/16/07; revised 5/20/07; accepted 6/12/07.

Grant support: A program for the Promotion of Fundamental Studies in Health Sciences of the Pharmaceuticals and Medical Devices Agency; a Health and Labour Science Research grant from the Ministry of Health, Labor and Welfare, Japan; and a Grant-in-Aid for Young Scientists from the Ministry of Education, Culture, Sports, Science and Technology, Japan.

The costs of publication of this article were defrayed in part by the payment of page charges. This article must therefore be hereby marked *advertisement* in accordance with 18 U.S.C. Section 1734 solely to indicate this fact.

Note: This study was presented at the 42nd Annual Meeting of the American Society of Clinical Oncology, Atlanta, Georgia, June 2-6, 2006.

Requests for reprints: Yuichiro Ohe, Division of Internal Medicine, National Cancer Center Hospital, 5-1-1 Tsukiji, Chuo-ku, Tokyo 104-0045, Japan. Phone: 81-0-3-3542-2511; Fax: 81-0-3-3542-6220; E-mail: yohe@ncc.go.jp.

doi:10.1158/1078-0432.CCR-07-0627

Table 1. Patient characteristics (N = 212)

	n (%)
Age (y).	
Median (range)	62 (29-84)
Sex	
Women	92 (43)
Men	120 (57)
Smoking history*	
Never smokers	96 (45)
Former smokers	38 (18)
Current smokers	78 (37)
Histology	
Adenocarcinoma	193 (91)
Others	19 (9)
Performance status†	
0	59 (28)
1	123 (58)
2	22 (10)
3	8 (4)
Stage	
III	42 (20)
IV	75 (35)
Recurrence after surgery	95 (45)
Gefitinib therapy	
First line	89 (42)
Second line	66 (31)
Third or more line	57 (27)

*Never smokers were defined as patients who have never had a smoking habit and former smokers were defined as patients who had stopped smoking at least 1 y before diagnosis.
†At the beginning of gefitinib therapy.

instruments and cost time and money. Recently, high-resolution melting analysis (HRMA) using the dye LCGreen I (Idaho Technology) was introduced as an easy, quick, and precise method for mutation screening (9), and we established a method for detecting DEL and L858R mutations using HRMA. Our cell line study revealed that DEL and L858R mutations could be detected using HRMA in the presence of 10% and 0.1% mutant cells, respectively (10). We also showed that the two major mutations could be identified by HRMA using DNA extracted from archived Papanicolaou-stained cytologic slides with 88% sensitivity and 100% specificity (10).

In this study, we validated *EGFR* mutation detection by HRMA using DNA extracted from archived paraffin-embedded tissues. We also did the HRMA in advanced NSCLC patients treated with gefitinib on a larger scale using archived tissues and/or cytologic slides.

Patients and Methods

Patients. Among 364 consecutive patients with NSCLC who began receiving gefitinib monotherapy (250 mg/d) at the National Cancer Center Hospital between July 2002 and December 2004, 212 patients were retrospectively analyzed using HRMA. One hundred fifty-two patients were excluded from the analysis because tumor samples were not available (n = 126) or their informed consent to the genetic analysis was not obtained (n = 26).

High-resolution melting analysis. On a protocol approved by the Institutional Review Board of the National Cancer Center Hospital, we did the following genetic analyses. Formalin-fixed, paraffin-embedded tissues and/or Papanicolaou-stained cytologic slides containing sufficient tumor cells (at least 1% of nucleated cells) were selected after microscopic examination by a pathologist (K.T.). The detailed analysis method has been described previously (10). Briefly, DNA was extracted from the tissues and/or cytologic slides using a QIAamp DNA Micro kit (Qiagen). PCR was done using dye LCGreen I and primers designed to amplify a region containing E746-I759 of *EGFR* [DEL-specific primer, AAAATTCCCGTCGCTATC (forward) and AAGCAGAAACTCACATCG (reverse)] or L858 of *EGFR* [L858R-specific primer, AGATCACA-GATTTTGGGC (forward) and ATTCTTTCTCTTCCGCAC (reverse)] on a LightCycler (Roche Diagnostics). The PCR products were denatured at 95°C for 5 min and cooled to 40°C to form heteroduplexes. The LightCycler capillary was then transferred to an HR-1 (Idaho Technology), a HRMA instrument, and heated at a transition rate of 0.3°C per second. Data were acquired and analyzed using the accompanying software (Idaho Technology). After normalization and temperature adjustment steps, melting curve shapes from 78.5°C to 85.5°C were compared between samples and control samples. Human Genomic DNA (Roche Diagnostics) was used as a control sample with wild-type (WT) *EGFR*. Samples revealing skewed or left-shifted curves from those of control samples were judged to have mutations. All analyses were done in a blinded fashion.

Table 2. Clinical validation of HRMA and direct sequencing without laser capture microdissection

	HRMA without LCM			Direct sequencing without LCM (6)
	Formalin-fixed tissues	Methanol-fixed tissues	Cytologic slides (10)	
n	66	66	29	66
Successfully analyzed, *n* (%)	63 (95)	66 (100)	28 (97)	66 (100)
True positive	34	36	14	28
True negative	26	29	12	29
False positive	0	0	0	0
False negative	3	1	2	9
Sensitivity (%)	92	97	88	76
Specificity (%)	100	100	100	100
Positive predictive value (%)	100	100	100	100
Negative predictive value (%)	90	97	86	76

NOTE: The results of these analyses were compared with those of direct sequencing with LCM (used as the "gold standard" method). True positive is defined as the correct detection of deletional mutations in exon 19 or L858R.
Abbreviation: LCM, laser capture microdissection.

Table 3. *EGFR* mutations among patient subgroups

	n	*EGFR* mutations				*P*
		DEL	L858R	Total	%	
Total	207	49	36	85	41	
Sex						
Women	89	31	17	48	54	0.001
Men	118	18	19	37	31	
Smoking history						
Never smokers	93	30	19	49	53	0.002*
Former smokers	38	12	10	22	58	
Current smokers	76	7	7	14	18	
Histology						
Adenocarcinoma	189	48	35	83	44	0.007
Others	18	1†	1‡	2	11	

*Comparison between never smokers and others.
†Pleomorphic carcinoma.
‡Adenosquamous carcinoma.

Clinical validation of HRMA. Direct sequencing with and without laser capture microdissection had been done in 66 patients with recurrent NSCLC after surgery in the previous study (6). In these patients, HRMA was done using both formalin-fixed and methanol-fixed surgical specimens without laser capture microdissection, and the results were compared with the results of direct sequencing with laser capture microdissection, which we considered to be the gold standard method.

Radiologic evaluation. One board-certified radiologist (U.T.) who was unaware of the patients' mutational statuses reviewed the baseline, the first follow-up, and confirmatory imaging studies and classified the tumor responses into complete response (CR), partial response (PR), stable disease (SD), and progressive disease (PD) using standard bidimensional measurements (11). In patients without measurable lesions, significant clinical benefit and disease progression were defined as clinical PR and clinical PD, respectively. Patients who died before the follow-up imaging studies were classified as PD. SD was subdivided into minor response (MR), long SD, and short SD. MR was defined as a ≥25% decrease in the sum of the products of the perpendicular diameters of all measurable lesions, and long SD meant that SD lasted for >6 months. Responders were defined as patients with CR, PR, or clinical PR.

Statistical analysis. The associations among *EGFR* mutations, patient characteristics, and tumor responses to gefitinib were assessed using a χ^2 test. The differences in time-to-progression and overall survival according to the patient subgroups were compared using Kaplan-Meier curves and log-rank tests. The starting point of the time-to-progression and overall survival was the first administration of gefitinib. Multivariate analyses using logistic regression models and Cox proportional hazard models were done to assess the association between the clinical outcomes and the following factors: age (<70 versus ≥70 years), sex, smoking history (never smokers versus others), histology (adenocarcinoma versus others), performance status (0/1 versus 2/3), stage (recurrence after surgery versus III/IV), prior chemotherapy (yes versus no), and the mutational status of *EGFR* (mutant versus WT). All analyses were done using the SPSS statistical package (SPSS version 11.0 for Windows; SPSS, Inc.).

Results

Patient characteristics. The patient characteristics are listed in Table 1. All the patients were East Asians: 210 Japanese, 1 Korean, and 1 Chinese. The median follow-up time for the survivors was 29.7 months (range, 10.7-49.8 months).

Clinical validation of HRMA. The clinical validation of the HRMA results using various samples is shown in Table 2. The sensitivity of HRMA using DNA extracted from formalin-fixed tissues was 92%, significantly higher than that of direct sequencing without laser capture microdissection but lower than that of HRMA using methanol-fixed tissues. The specificity and positive predictive values were 100% in all the analyses.

Mutational analysis. HRMA was completed in 207 patients. Five patients could not be successfully analyzed because of incomplete PCR. Of the 207 patients, 130 were analyzed using tissue samples (96 samples were obtained by thoracotomy, 17 by mediastinoscopic lymph node biopsy, 9 by thoracoscopic lung or pleural biopsy, 5 by resection or biopsy of distant metastases, and 3 by transbronchial lung biopsy), and 117 were analyzed using cytology samples (43 samples were obtained by bronchial brushing or washing, 40 from pleural effusion, 9 by transbronchial needle aspiration, 8 from pericardial effusion, 7 by needle aspiration of superficial lymph nodes, 6 by percutaneous needle aspiration of lung tumors, and 4 from sputum). In 40 patients who were analyzed using both tissue and cytology samples, 4 had inconsistent results; mutations were detected only in tissue samples and not in cytology samples (3 patients) or vice versa (1 patient). These four patients were judged to have mutations because false-negative results were more common than false-positive results in the validation of HRMA. Consequently, DEL and L858R mutations were detected in 49 (24%) and 36 (17%) patients, respectively, and these mutations were mutually exclusive. The other 122 (59%) patients were classified as having WT *EGFR* in this study, although some of them may have had minor mutations. As

Table 4. *EGFR* mutations and response to gefitinib

	Responders		SD			PD	Response rate (%)	*P*
	CR	PR	MR	Long SD	Short SD			
WT	0	10	2	4	17	89	10/122 (8)	$<10^{-23}$
Mutant	2	64*	6	4	1	8†	66/85 (78)	
DEL	0	42	2	2	1	2	42/49 (86)	0.037
L858R	2	22	4	2	0	6	24/36 (67)	
Total	2	74	8	8	18	97	76/207 (37)	

*Including four clinical responders without measurable lesions.
†Including a patient who had no measurable lesions at baseline.

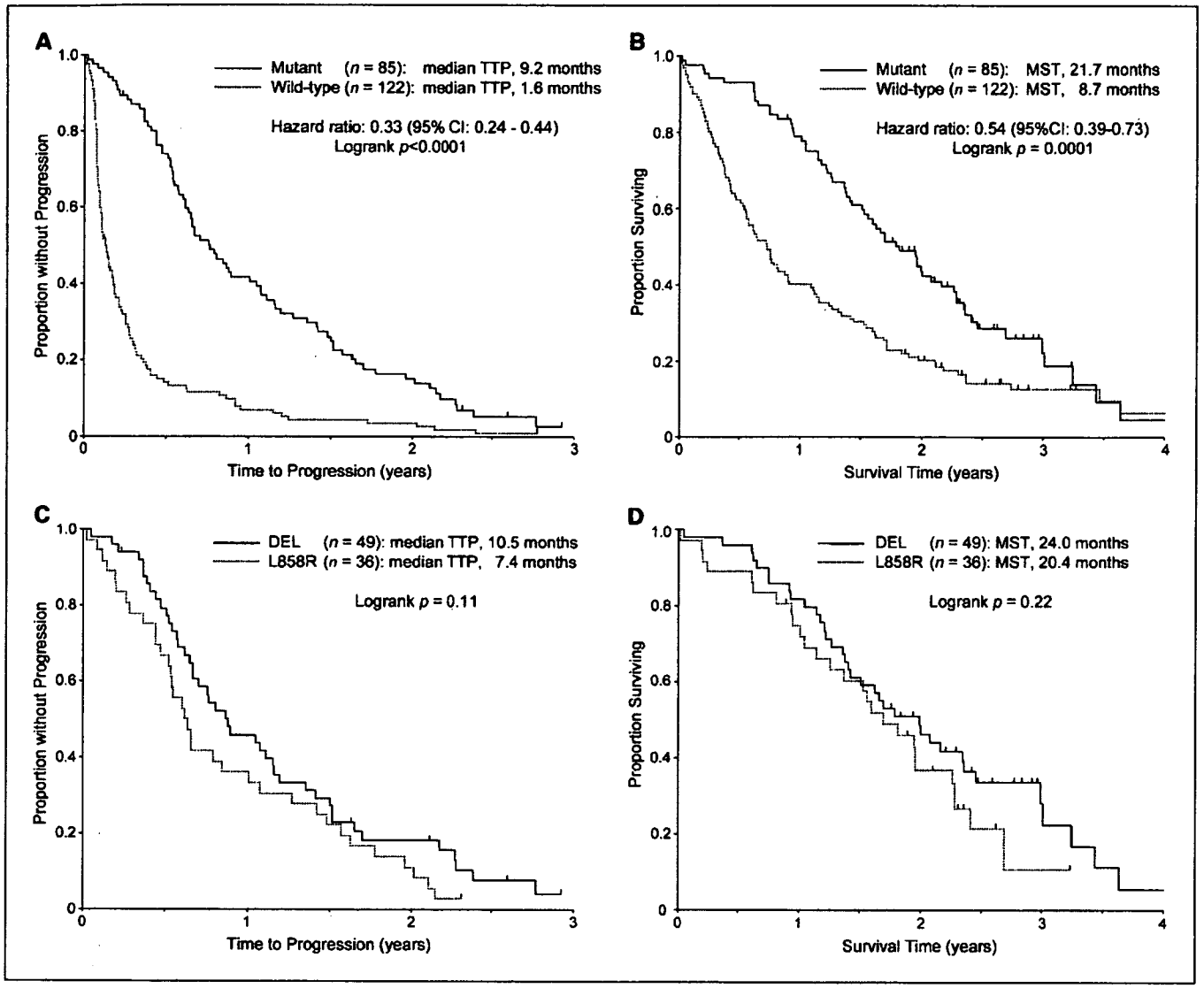

Fig. 1. Kaplan-Meier plot of time-to-progression (*A*) and overall survival (*B*) for patients with or without *EGFR* mutations. Kaplan-Meier plot of time-to-progression (*C*) and overall survival (*D*) for patients with DEL or L858R mutations. TTP, time-to-progression; MST, median survival time.

shown in Table 3, *EGFR* mutations were detected more frequently in women, never smokers, and patients with adenocarcinoma. Patient characteristics were not significantly different between patients with DEL mutations and those with an L858R mutation.

EGFR mutations and clinical outcomes. The association of the mutational status of *EGFR* and the response to gefitinib is shown in Table 4. The response rate was significantly higher in patients with *EGFR* mutations than in those with WT *EGFR* (78% versus 8%; $P < 10^{-23}$). Among patients with *EGFR* mutations, those with DEL mutations had a higher response rate than those with an L858R mutation (86% versus 67%; $P = 0.037$). Tumor responses were classified as SD in 11 patients with *EGFR* mutations and in 23 patients with WT *EGFR*. Among the patients with SD, a MR and/or a long SD (>6 months) were observed more frequently (91% versus 26%; $P = 0.0004$) and the time-to-progression was significantly longer (median, 6.9 versus 4.4 months; $P = 0.019$) in the patients with *EGFR* mutations than in the patients with WT *EGFR*.

As shown in Fig. 1, the time-to-progression (median, 9.2 versus 1.6 months; $P < 0.0001$) and overall survival (median, 21.7 versus 8.7 months; $P = 0.0001$) were significantly longer in patients with *EGFR* mutations than in those with WT *EGFR*. Patients with DEL mutations tended to have a longer time-to-progression (median, 10.5 versus 7.4 months; $P = 0.11$) and overall survival (median, 24.0 versus 20.4 months; $P = 0.22$) than those with an L858R mutation, although the difference did not reach statistical significance.

Clinical outcomes among subgroups of patients are shown in Table 5. In the univariate analysis, sex, smoking history, and histology were significant predictive factors for gefitinib sensitivity.

In the multivariate analyses, the mutational status of *EGFR* was an independent predictive factor of response [odds ratio, 38.9; 95% confidence interval (95% CI), 15.7-96.5; $P < 0.001$], time-to-progression (hazard ratio, 0.33; 95% CI, 0.24-0.45; $P < 0.001$), and overall survival (hazard ratio, 0.48; 95% CI, 0.34-0.67; $P < 0.001$). A poor performance status (2/3) was an